KTH Chemical Engineering
and Technology

Fabrication of Polymeric Microfluidic Devices via Photocurable Liquid Monomers

Klas Tommy Haraldsson

Doctoral Thesis 2005

KTH- Royal Institute of Technology
Department of Chemical Engineering and Technology
Fibre and Polymer Technology
Stockholm, Sweden

Contact information:
Address: KTH Department of Fiber and Polymer Technology
Polymer Technology
Royal Institute of Technology
Teknikringen 56-58
SE 100 44 Stockholm
Sweden

Cover image: 3D microfluidic maze
fabricated via CLiPP.

Printed by Universitetsservice US AB
Stockholm, Sweden, 2005

TRITA-FPT-Report 2005:26
ISSN 1652-2443
ISRN KTH/FPT/R-2005/26-SE
ISBN 91-7178-183-8

Abstract

Keywords: Photopolymerization, radical photopolymerization, polymerization kinetics, photoinitiation, vinyl ether, maleate, vinyloxy, contact liquid photolithographic polymerization, CLiPP, photolithography, microfluidic, microfluidics, microfluidic devices, micropatterning, DTC, dithio carbamoyl, living radical, living radical photopolymerization, LRPP, undercut structures, sacrificial material, surface modifications, permanent surface modifications, grafting, covalent bonding.

Microfluidic devices have long been considered an ideal tool for rapid and inexpensive chemical analysis and reactions in areas ranging from point-of-care health to national security applications. However, fabricating microfluidic devices is time consuming, difficult and above all expensive. In commercial applications many thousand units need to be sold before the development costs are recovered. The problem is compounded since most microfluidic devices do not have generalized architectures which means that each end use requires a specialized design. The microfluidics marketplace can therefore be seen as being composed of 1000's of niche markets.

To address development costs, there is clearly a need for a versatile technology that can be used for many different applications and that enables rapid testing and optimization of new designs. This work describes such a technology: Contact Liquid Photolithographic Polymerization (CLiPP).

The thesis consists of two parts: polymerization kinetics and the fabrication of polymeric microfluidic devices via CLiPP.

The photopolymerization kinetics is evaluated for a number of monomer types, and the results are used to assess their suitability in the CLiPP process. Vinyl ether/maleate photoinitiated copolymerization is examined in detail. It is shown that the polymerization kinetics is dramatically influenced by the availability of easily abstractable hydrogens The presence of α-hydrogens adjacent to the vinyl ether functional group reduces the polymerization rate and the dependence of the polymerization rate as a function of initiation rate. Also, photoinitiated acrylate and methacrylate polymerization kinetics are presented. The kinetics results in these three monomer types are used to explain the different patterning properties of the monomer functionalities used in the CLiPP process, in which acrylates show enhanced patterning properties compared to methacrylates.

The polymerization kinetics is studied with traditional tools and methods: photo Differential Scanning Calorimetry (photo-DSC), photo Fourier Transform Real Time Infrared Spectroscopy (photo-RTIR), and photo Real Time Electron Paramagnetic Spectroscopy (ESR).

The microfluidic fabrication is performed via both in-house fabricated and commercially available CLiPP-specific hardware. The patterning qualities of the structures are evaluated via Scanning Electron Microscopy (SEM) and Optical Microscopy. The finished devices are used in their intended environment and evaluated in suitable manners to assess their utility.

In this thesis, the development and design of specialized CLiPP fabrication machines, fabrication techniques and resulting microfluidic device features are presented and

discussed. It is shown that the CLiPP scheme enables features such as 3 dimensional (3D) capabilities for minimized device footprints, a very large number of polymeric materials for optimized device components as well as facile integration of prefabricated components. Also, covalent layer adhesion and permanent surface modifications via living radical processes are demonstrated. These capabilities are exemplified in a number of examples that range from a 3D fluidic channel maze with separated fluidic streams and a device with independently moveable parts to a device constructed from multiple polymeric materials and devices with permanently modified surfaces, Also, batch processing capabilities are shown through fabrication of 400 identical undercut microstructures

Rapid and inexpensive design evaluations, multiple materials capabilities and the ability to seamlessly incorporate prefabricated microstructures of the CLiPP process strongly encourages continued method development. The future work that remains to be addressed is divided into two parts. First, to enable novel research devices, new polymer materials with enhanced mechanical and surface properties must be developed. Also, integration of prefabricated microstructures such as sensors and actuators has to be incorporated in a reproducible and rational manner. Secondly, to enable device mass fabrication, new automated equipment is to be developed in order to utilize the full batch processing potential of CLiPP.

Sammanfattning

Mikrofluidik-komponenter har länge betraktats som perfekta verktyg för att snabbt och kostnadseffektivt utföra kemiska analyser och reaktioner i varierande miljöer. Läkarmottagningar, tull och polis anses vara speciellt lämpade för mikrofluidik-komponenter. Tillverkning av mikrofluidik-komponenter är dock komplex, tidskrävande och framför allt dyr. I kommersiella applikationer måste tusentals enheter säljas för att betala utvecklingskostnaderna. Dessutom, eftersom varje mikrofluidik-komponent är unik förekommer det få mikrofluidiklösningar i massproduktion.

De höga utvecklingskostnaderna måste reduceras innan ett större marknadsgenomslag för mikrofluidiklösningar kan komma till stånd. För detta krävs nya tillverkningstekniker, både för utvecklingsarbete och massproduktion. I den här avhandlingen beskrivs en mikrofabrikationsteknologi, Contact Liquid Photolithographic Polymerization (CLiPP), med potential att lösa många av de problem som nuvarande metoder har.

Avhandlingen består av två huvuddelar: polymerisationskinetik och mikrofluidik-komponenters framställning genom CLiPP.

Fotopolymerisationskinetiken för olika monomertyper har studerats och resultaten har använts för att utreda deras användbarhet i CLiPP-metoden. Av det tre monomertyperna har de sampolymeriserande vinyl eter/maleat-monomerernas polymerisationskinetik utretts i detalj. Det visas att tillgängligheten på abstraherbara väten är en mycket viktig förklaring för den uppvisade kinetiken. Tillgång på abstraherbara α-väten minskar polymerisationshastigheten och polymerisationshastighetens beroende av initieringshastigheten. Fotopolymerisationskinetik för akrylater och metakrylater presenteras också. Kinetikresultaten används för att förklara kvaliteten på mönster-replikationsprocessen för dessa tre monomerer.

Polymerisationskinetiken har studerats med foto-kalorimetri (foto-DSC), foto-realtids Fourier Transform IR (foto-RTIR) och foto-realtids elektronspinnresonans (ESR).

För att tillverka mikrofluidik-komponenter har uppställningar tillverkade både av universitet och en professionell instrumenttillverkare använts. Med hjälp av svepelektron-spektrokopi (SEM) och ljusmikroskopi har mikrofluidik-komponenternas kvalitet och struktur utvärderats. Dessutom har de färdiga kompnenterna studerats med metoder speciellt avsedda för att kunna bedöma deras användbarhet i riktiga applikationer.

Instrumentutveckling och -design, fabrikationstekniker och färdigställda mikrofluidik-komponenter presenteras och utvärderas. I avhandlingen visas att CLiPP-metoden möjliggör tillverkning av tredimensionella komponenter med en optimerad ytanvändning, många olika polymera material för speciellt anpassade komponentstrukturer samt enkel integration av olika förtillverkade komponenter. Vidare visas hur levande radikalprocesser används till kovalenta bindningar mellan olika komponentlager samt permanent ytmodifiering via graftning. CLiPP är en batchprocess, vilket visas genom ett exempel där fyrahundra identiska mikrostrukturer har tillverkats.

Den snabba och kostnadseffektiva utvärderingen av mikrofluidik-komponenters funktion och den enkla integrationen av olika förtillverkade komponenter gör att fortsatt metodutveckling är attraktiv. Framtida utvecklingsarbete kan delas in i två huvudfåror: 1) För forskningsapplikationer är nya polymera material, ytmodifieringar samt integration av

elektronik viktiga, medan för 2) massproduktion måste nya CLiPP-instrument framställas för fullt utnyttjande av kapaciteten hos batchtillverkning.

List of Appended Papers

This thesis is a summary based on the following papers, referred to by Roman numerals I- V.

I. **Robust Polymer Microfluidic Device Fabrication via Contact Liquid Photolitographic Polymerization (CLiPP)**
Hutchison J., Haraldsson K., Good B., Sebra R., Luo N., Anseth K., Bowman C., 2004, Lab on a Chip, pp. 658-662.

II. **3D Polymeric Microfluidic Device Fabrication via Contact Liquid Photolithographic Polymerization (CLiPP),**
Haraldsson K., Hutchison J., Sebra R., Good B., Anseth K., Bowman C., Sensors and Actuators B, in press.

III. **The Effects of Hydrogen Abstraction on the Kinetics of Monofunctional Maleate/ Vinyl Ether Radical Photopolymerizations**
Haraldsson K., Johansson M., Bowman C., Hult A., manuscript

IV. **The Role of Abstractable Hydrogen in Radical Photopolymerization of Maleate/ Vinyl Ether Monomers Studied With EPR and Photo-RTIR**
Haraldsson K., Johansson M., Hult A., manuscript

V. **Fabrication of a Geometrically Complex Brain Slice Perfusion Device via Contact Liquid Photolithographic Polymerization (CLiPP)**
Haraldsson K., Passeraub P., manuscript

My contribution to the appended papers:
I am the main author of the papers listed above, except for Paper I. The majority of the experimental work in Paper I was conducted by me. In Paper V the design and testing of the brain slice perfusion device was conducted by Philippe Passeraub, while I performed the adaptation of the design and the fabrication work. In the other Papers, I did all experimental work.

My contribution to CLiPP:
I am the inventor and main developer of the CLiPP fabrication techniques, i.e. single layer and multilayer device fabrication, incorporation of prefabricated structures, and initial materials development, reported in this thesis and the designer of the first two CLiPP tooling sets.

The use of the CLiPP-specific living radical chemistry for polymeric network polymerization was invented by Chris Bowman, developed by Brian Hutchison and Ning Luo, and further developed and adapted to a biotechnological context by Robert Sebra, all at the University of Colorado (CU).

The use of non-polymeric materials for conductivity and heating was developed by Brian Good, CU.

My contribution to CLiPP is further reflected in the status as corresponding inventor on the patent application covering the fundamentals of the CLiPP process: Haraldsson, K. T.; Hutchison, J. B.; Anseth, K. S.; Bowman, C. N. U.S. PCT filed patent application 60/397215. 2002.

Table of Contents

1. Introduction

1.1. Miniaturization

Miniaturization lies at the core of many of today's scientific advances. Particularly the electronics industry has benefited from improved microscale technologies and the field of integrated circuits (IC) has been created from miniaturization breakthroughs.

Not only the IC industry has focused on miniaturization, but other fields have been targeted as well. In fact, all information gathering and data processing operations are suitable for miniaturization since, in principle, the results are independent of the amounts of reagents or energy that are expended in the process.

A couple of decades ago, pioneers started miniaturizing classical lab operations such as mixing, chemical reaction containment and fluidic handling. In miniaturized labs, or *microfluidic devices,* chemical reactions and detection operations are performed to obtain results using the smallest amount of reagents and samples as possible.

In Figure 1 the parallels between microelectronics and microfluidics are apparent. In Figure 1 **a)** a typical electronics wafer is shown and in **b)** fluidic logics operations for improved sample and reagent controllability using innovative valving techniques is presented. [1]

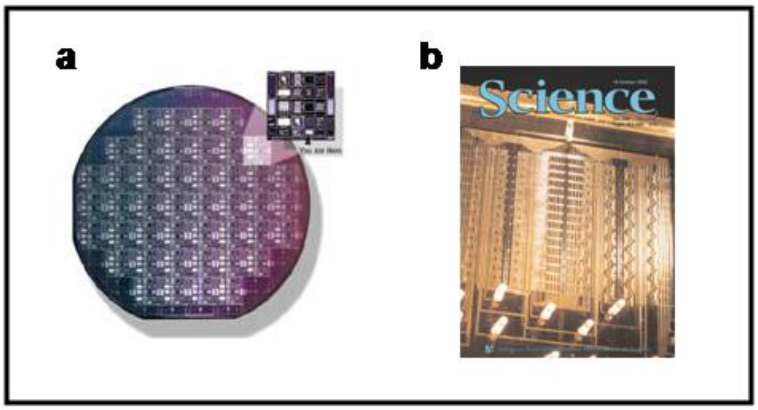

Figure 1 Microelectronics and microfluidics compared. ***a)*** *A typical wafer with individual integrated circuits laid out. Picture from Intel Corporation.(http://www.intel.com)* ***b)*** *the cover of Science journal where a large scale fluidic logics circuit is displayed.*

The parallels between IC and microfluidics extend one step further. For electronics performance, minimized distance between transistors is paramount, and in microfluidics smaller size scales enable more unit operations, e.g. pumps, valves and mixers, to fit on the same chip. This in turn enables more complex functions and shorter reaction times.

1.2. Objectives of the Thesis

The main objective of this work is to develop a novel fabrication technology for fully polymeric microfluidic devices. The technology is to address limitations in current state-of–the-art microfabrication techniques in terms of materials selection, geometrical capabilities and compatibility with microcomponents fabricated with other techniques.

The fabrication work will be conducted with newly developed technologies and hardware, and the devices produced will either prove a principle or be directly useful in a biotechnical context.

1.3. Thesis Outline

This thesis is based on five appended papers that range from kinetics of vinyl ether-maleate copolymerizing formulations to the ultimate utility of these formulations in the novel Contact Liquid Photolithographic Polymerization (CLiPP) process.

The structure of the thesis is somewhat different from what the reader may be used to due to the cross-disciplinary nature of the topic. Two separate introductions are made. First, the one into the field of microfluidics, Chapter 2 and state of the art fabrication schemes for microfluidics, Chapter 3. Secondly the one into the field of photopolymerization, which constitutes the beginning of Chapter 4, is made. These chapters will benefit readers that are proficient in one of these disciplines, i.e. photopolymerization or microfluidics. The referencing follows the same ambition, and many of the works cited are reviews or books that give a good understanding of the progress in the particular field or application cited.

The results chapters differ to those commonly found in dissertations based on articles, since many results not mentioned in the appended papers are included. This is primarily due to the novelty of the method where many interesting partial results that are not sufficient for full papers still warrant description for a more comprehensive picture. Some critical components in the CLiPP process that have been explored by other researchers at the University of Colorado are included in the thesis for reasons of context and understandability, see the list of appended papers. Also, device figure captions indicate the main contributor in terms of design and fabrication.

Chapter 5 describes the CLiPP process, from a development perspective, via tooling considerations. This chapter is based on Papers I and II.

Chapter 6 details how advanced undercut geometries are fabricated (Paper II) and the role of surface initiation, both for adhesion and surface modifications (Paper I).

Chapter 7 deals with factors that affect patterning in the CLiPP process, coupling previous kinetics results and considerations presented in Chapter 4 to CLiPP, which is presented in Chapter 5.

Chapter 8 is based on Paper V and shows how the technology is applied to a real-life biomedical application.

Conclusions from this work are presented in Chapter 9.

Finally, in Chapter 10, future work in CLiPP method development needed for applications in research and commercial endeavors are discussed.

2. Background to Microfluidics

The purpose of this chapter is to provide a background to microfluidics and the particular scaling laws that govern the microworld. The advantages and current uses of microfluidic solutions are introduced and a brief outlook into microfluidic markets and trends is discussed.

2.1. Microfluidics

A number of attempts to define microfluidics have been made and most tentative definitions state that microfluidic devices contain channels that are in the subμm to 1 mm range with fluidic volumes of nanoliters.

Initially, microfluidic devices were often simple channel geometries that allowed for a few chemical reactions on a glass chip. Current microfluidic devices are far more complex with entire laboratory protocols shrunk down to only a few cm^2. To reflect this increased chip complexity, two new names have been coined; "lab on a chip" and "micro-total analysis systems" (μTAS).

The term "lab on a chip" is quite descriptive since microfluidics and standard laboratory protocols are closely related, both in terms of chemical reactions and reaction conditions. When more closely compared, however, differences between micro and macro are readily apparent, where microfluidic devices have shorter reaction times, yield is higher and reagent consumption is much reduced. Thus, there is a very large incentive to design microfluidic devices that replace macroscopic protocols for chemical reactions and molecular manipulations. The reason that microfluidic devices are not commonplace is that successful designs require intense development and large resources, both in terms of man-hours and equipment. Despite this, large sums have been invested in microfluidics technologies since it is widely realized that the advantages of microfluidics outweigh the drawbacks. Indeed, microfluidics has taken a small but important place in diverse areas such as drug discovery and drug screening[2], disease detection[3], proteomics[4] and genomics research[5].

2.1.1. Microscale Phenomena

The world of microfluidics is quite different from the everyday macro-world we experience. Most differences are attributable to relative changes in volume and surface area when the sizes are diminished. A number of so-called scaling laws that relate the macro and microworld have been developed for important properties such as, inertia, surface tension and heat transfer. The following summary is limited to fluidic, thermal and mechanical behavior, but similar considerations have been given to electric and magnetic scaling.[6]

Surface-to volume-ratio (S/V)

The overall effect of changing the scale is a shift in the importance of phenomena that rely on the volume, which scales to the cube, or on the area, which scales to the square. Thus,

as dimensions decrease, area dependent frictional forces start to dominate over volume dependent inertial forces. Hence, standard moveable macrocomponents, such as cogwheels, flywheels and valves, behave very differently in the microscale. To ensure moveability, the contacting surfaces need to be very smooth and the stiction, i.e. sticking due to van der Waals forces and/or polar forces, needs to be minimized through careful materials selection. While many interesting analogs to macroscale equipment have been made, e.g. see Figure 2, devices that benefit from the increase in surface to volume ratio, rather than fighting its consequences, are generally more successful.

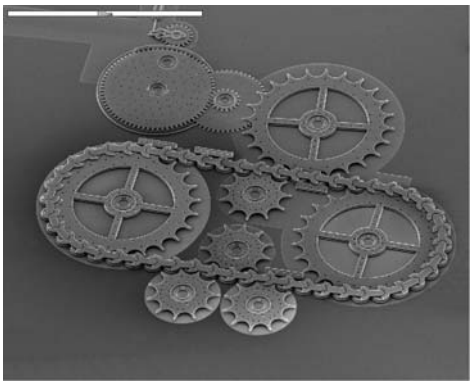

Figure 2 The worlds smallest chain drive, designed and built at Sandia National Labs, NM, USA. The scale bar on top is 500 μm. (http://www.sandia.gov)

From a fluidics standpoint, diffusion distances of dissolved molecules are sufficiently small to increase the chance that molecules interact with channel walls. This is desirable in surface detection schemes, but most often adsorption is unwanted since the sample concentration is lowered, perhaps even below the detection limit.

Heat transfer

The short distance between a heating elements and a liquid plug flowing in a channel ensures very rapid and localized heating. Cooling is also very fast. As the heated liquid plug moves away from the heating source, the small liquid volume, in contact with a relatively large surface, ensure rapid cooling. Multiple temperature steps can therefore be closely packed in a single channel.. The polymerase chain reaction (PCR) lab-on-a-chip is a good example of rapid thermal cycling for enzymatic reactions.[7]

Prevalent laminar flow

Typically, the fluids in microfluidic applications are liquids and not gases. Due to the high viscosity of most liquids the Reynolds number is low[7], with typical values of $Re < 1$. Flow profiles are therefore laminar in microfluidic streams. The most obvious consequence of laminar flow is poor mixing since only diffusion serves to mitigate concentration differences. The issue of mixing has garnered much attention, and a large number of mixing schemes have been designed: simply very long 2D channels, 3D tortuous flow paths[8], herring bone structured channel bottoms to impose chaotic flow,[9]

formation of microbubbles in an incompatible liquid[10] and specially designed plugs with numerous tortuous paths throughout the structure.[11]

2.1.2. Benefits of Microfluidics

Some benefits of microfluidics have already been described in the sections above. Since the examples are spread throughout the text a summary with the main advantages is useful:

- *Significant decrease in reagent consumption and waste generation*: The small volumes and low concentration requirements due to increased sensitivity of detection schemes, allow for very small amounts of reagents.
- *Decreased cost per analysis:* The decreased cost per analysis is mainly due to low reagent consumption. With new efficient fabrication technologies, the cost per device will also be low.
- *Results of analyses in a few seconds:* The small volumes needed and the close proximity of target and analyte molecules ensure rapid analysis.
- *Allows chemists to carry out reactions that are impossible in the macro-world:* Certain reactions and crystallizations are carried out much more efficiently in microfluidic devices than in other techniques, even to the extent of allowing for schemes that are impossible to carry out in using macroscopic equipment.[12]
- *Improved control of reaction environment in chemical reactions:* The enclosed environment of most microfluidic devices is easily controlled since only very limited exchanges with the ambient are allowed.
- *Enables portable analysis systems:* The small size of microfluidic devices enables portable systems if the power requirements of the detection schemes employed are sufficiently low.

The above advantages have been capitalized on by numerous research groups and companies and vast array of devices have been fabricated. However, the reasons for these advantages, i.e. the scale down, also pose some serious difficulties. Some of these are discussed in the next section.

2.1.3. Microfluidic Challenges

Transforming macro to micro is costly. Design and, particularly, fabrication is both difficult and expensive, often requiring specialized non-standardized fabrication processes. The primary challenges for microfluidics are geometrical, i.e. issues that relate to unit operations at a small scale, and surface chemistry related:

Geometrical issues

- *Microfluidic interconnections, i.e. chip-to-world interfaces*: Microfluidic interconnections require that the fabrication method allows for large structures while still able to reproduce μm sized patterns.
- *Mixing can only be performed by diffusion, due to laminar flows*: If mixing is required, channels need to be of sufficient length to allow for molecular diffusion at an acceptable flow rate. Thus, the fabrication method needs to allow for either efficient channel packaging, possibly through the use of 3 dimensional designs,[8] or specialized unit operations that promote mixing, e.g forced directional changes.[9,11]
- *Large capillary forces:* Small channels lead to large capillary forces, which may drive fluids into unwanted areas of the device, risking contamination of other fluid streams.
- *Possible evaporation:* At small scales, the surface to volume ratio is large. Thus, fluids exposed to the surroundings rapidly evaporate.

Surface chemistry issues

- *Adsorption of dissolved molecules:* Adsorption depend to some extent on channel length, but is primarily a function of surface chemistry. Dissolved molecules that encounter a surface with a high specific binding constant will reside for some time before re-entering the stream, which reduces the concentration of the sample "plug" that is carried along the channel
- *Clogging and blocking:* Clogging is severe adsorption over a long period of time, and may cause bottlenecks and even blocking of channels.

For more complex devices many of these challenges are combined, which leads to design and fabrication difficulties.

2.1.4. Demands on Microfluidic Devices

The demands put on microfluidic devices originate from the challenges listed above. The old proverb "the chain is not stronger than its weakest link" is appropriate for microfluidics, since all relevant demands must be met in a single device, or it simply will not function to specifications.

2.1.5. Microfluidic Applications

In the 1980's, microfluidic phenomena were first explored, and prototype microfluidic devices were described and tested. Initially, researchers concentrated on mimicking large scale unit operations, simply shrinking the size scales. As has been pointed out earlier, it soon became clear that microfluidics offered more than merely a reduction in size, due to the scaling laws. Innovative solutions for mixing, heating and surface modifications soon appeared. It also became clear that microfluidic features were well suited for adaptation of advances made in other expansive research fields, in particular biotechnology.

Microfluidics is used in lab intensive applications, such as drug discovery and drug screening. Applications have now reached a sufficiently advanced stage to replace animal models, e.g. rat experiments, in some instances with single cell studies.[13] This is obviously beneficial to the animals while simultaneously reducing research time and cost.

Other fields where microfluidics has made inroads is in bioassays such as DNA sequencing, polymerase chain reaction (PCR), electrophoresis, DNA separation, enzymatic assays, immunoassays, cell counting, cell sorting, and cell culture.[14,15,16] Also microfluidics is making headways into proteomics both for the elucidation of protein structures and more recently to detect small quantities of specific proteins in biological samples.[17]

2.2. Microfluidic Markets

Both military (including national security) and civilian markets are demanding smaller more integrated sensing and monitoring devices for biochemistry, gas analysis, and environmental monitoring. Microfluidic devices meet these requirements. Applications such as lab-on-a-chip, point-of-care-diagnostics, biomedical devices, disposable blood testing, and high-speed gas detection are part of the driving force for the new microfluidic device demand. According to market studies, the microfluidic market for life science applications reached $350 million in 2004 (source: Yole Development market Research) and is projected to grow to $2 billion by 2010. This includes in vitro diagnostics, drug discovery, and drug delivery. The sizeable market and exceptional growth projections ensure that continuing efforts into device fabrication and marketing will be pursued.

2.3. Current Trends in Microfluidics

The microfluidics community is moving in two different directions; simple microfluidic chips with increasingly advanced auxiliary bench-top equipment; and self contained lab-on-a-chip devices with increased functionality. So far, the first has been more commercially successful than the latter. Most of the growth reflected in the projected numbers above is thought to come from smaller, more complex, yet simpler to use, microfluidic devices. To reach the numbers, these solutions have to be adopted by medical professionals in large numbers. This breakthrough in the use of microfluidic devices has not been realized yet.

3. Background to Microfabrication Methods

In this chapter, microfabrication technologies are reviewed with particular emphasis on technologies for polymeric microdevice fabrication. This chapter is primarily for readers not familiar with microfabrication techniques, and serves as a background for later comparisons with the CLiPP process, which is presented in Chapter 5. Some strictly prototyping micromachining techniques, such as drilling, and Computer Numerical Control (CNC) machining, are not presented, even though they sometimes are useful for mold fabrication. Other microfabrication techniques require extremely expensive machinery, e.g. LIGA utilizes high energy synchrotron radiation, and are therefore deemed beyond the scope of this short introduction to micromachining. Madou's *"Fundamentals of Microfabrication"* [7] is an excellent introductory text to microfabrication and much of this chapter is based on information contained therein.

3.1. Microfluidic Device Materials

To date, microfluidic devices are primarily made from non-polymeric materials used in the Integrated Circuit (IC) industry, such as silicon and glass. Historically, the main reasons for this choice was an abundance of equipment, well established techniques and micropatterning know-how and the potential to merge micro fluidics with electronics. However, microfluidic devices are not computer chips, where tasks are solved with software on generalized hardware platforms. Pumps and valves do not scale like their electronic counterparts, which are composed of transistors in various logics configurations, so each microfluidic device has to be designed and fabricated in limited series tailored to specific purposes. The development cost for each device is thus prohibitively high. To address the problems with semiconductor based micromachining, a number of alternative fabrication methods have emerged. The most promising technologies involve forming and shaping polymers in various manners.[18,19]

Polymeric material's variability is almost infinite. They are lightweight and durable which is important for field portability and the moduli are varied to specific demands such as rough environments that require tough materials or low modulus for the construction of on-chip pumps etc.

3.2. Microfluidic Device Fabrication

While microfabrication techniques are increasingly versatile, there is not yet a technology that combines device utility with inexpensive and simple fabrication. This has been recognized by the European Union, which has supported an academia/industry initiative called 4M (Multi-Materials Micro Manufacture, http://www.4M-net.org). The main goal, over a number of years, is to stimulate and promote novel non-Silicon techniques for inexpensive and reliable micro- and nano-fabrication.

The remainder of the chapter will discuss common fabrication techniques and their main advantages and drawbacks.

3.2.1. Photolithography

In the IC industry, structures are created almost exclusively via photolithography, i.e. the transfer of energy via light for initiation of specific chemical reactions. The reasons are primarily due to convenience and cost. It is convenient since light is easily created and spatially controlled, and cost effective since the energy requirements are modest and necessary equipment is readily available. These advantages are also the reasons that photolithography is used for microfluidics fabrication of structures that are too small to be easily produced via micromilling or other mechanical micromachining techniques.

Photolithographic techniques

Photolithographic techniques are used for the fabrication of microdevices, either directly through feature patterning or indirectly through fabrication of molds that are subsequently used to shape thermoplastic materials or thermosetting formulations.

Photolithography relies on having a precursor, liquid or solid, that contains photoactive components that undergo a chemical change when exposed to certain wavelengths of light. Typically, the light effects a transition from liquid into a solid or effect changes in solubility. To avoid transforming all of the liquid in this manner, photomasks are used to block the light in desired areas. The photomask image is "transferred" to the reactive liquid upon light exposure. After rinsing protocols to remove the unconverted liquid precursor (for negative resists), there remains a pattern of solid material, which can be further added on or used to protect the surface from etchants etc. For positive resists, the dissolution is faster for exposed areas, which leaves unexposed areas on the substrate. There are advantages and disadvantages inherent in both positive and negative resist, and the ultimate desired pattern dictates which one is used. For microfluidics, negative resists such as EPON® SU-8, Shell Chemical Company, is typically preferred due to excellent mechanical properties and high aspect ratios.

Photolithography equipment

The basic component of any photolithographic system is the light source. For standard feature sizes, i.e. more than 1 μm, UV light of 254-365 nm is sufficient. This light is typically generated with medium pressure Hg-lamps similar to typical gas light bulbs. These wavelengths require no special optics, as opposed to X-rays, or evacuation of air since ozone is not created with wavelengths above 170 nm.

3.2.2. Spin Coating

One of the most versatile microfabrication technologies that have emerged from the IC industry is spin coating. In conjunction with photolithography, it is a means to selectively protect certain areas of a substrate with a thin layer of organic material.

Extensively developed over four decades, the spin coating and resist technologies have reached a maturity and prevalence that make them a natural choice for fabricating microstructures. Thus it is not surprising that spin coating of resists was the first technology used for microfluidic device fabrication and it is still used in many modern microfabrication schemes.

Spin coating basics

Spin coating allows for the application of a thin (1-500 μm) organic photoresist layer on a solid substrate through the application of a centrifugal force that spreads a liquid resist drop thinly across the substrate. After evaporation of any solvents in the resist formulation via soft baking, the organic layer is patterned using photolithography.

The spin coating process is shown schematically in Figure 3. In Figure 3 **a)** liquid photoresist is applied in the centre of the substrate. In Figure 3 **b),** the substrate is spun according to a preset schedule, often involving several different revolutions per minute (RPM) with ramp up and ramp down sequences between them. After soft baking to remove solvents (not shown), photolithography is used to impart chemical changes in transparent regions of the photomask, Figure 3 **c)**. After a post bake step that crosslinks the exposed regions (not shown) the final structure is released through preferential dissolution in a solvent bath of the unexposed regions, Figure 3 **d)**.

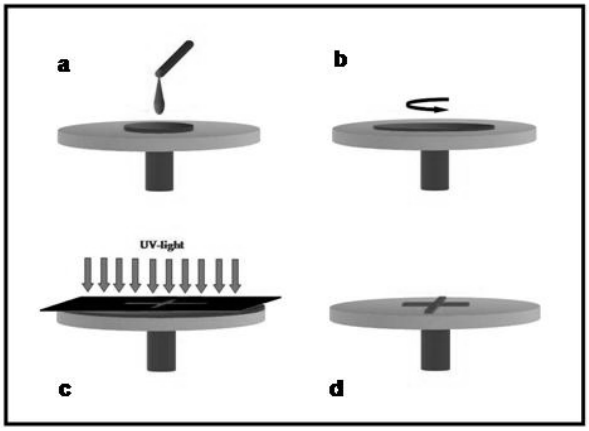

Figure 3 Spin coating process steps for the fabrication of a molding template.

Photoresists

There are two main types of photoresists: the positive resist that has an increased solubility in exposed areas and the negative resist that is insolubilized in exposed areas. The latter is far more common in microfluidic applications, and is used for direct fabrication of devices as well as for molds that are later used as a negative template for devices constructed from a different material. Mold use is shown in Section 3.4 for several replication techniques.

Microfluidics applications of spin coating

After the pattern is formed, there are two choices for fabricating vias, trenches and holes. First, there is the choice of letting the resist itself form the walls of the fluidic structures. Secondly, there is the choice of forming fluidic structures from the substrate by etching unprotected areas and subsequently strip the resist.

Advantages of spin coating

The main advantages of using photoresists for direct fabrication of microfluidic devices are relative ease of production and a standardized and well-known technology. Furthermore, it is often quoted that the resulting polymer is versatile due to its high crosslinking density, high modulus and temperature resistance. In some resists it is possible to fabricate very tall features with excellent aspect ratios (EPON® SU8: 500 μm in one coating and aspect ratios of up to 50).[20]

Disadvantages of spin coating

There are many disadvantages using this method. Firstly, it is difficult to achieve channels since forming a channel ceiling typically involves using green tape, i.e. prebaked photoresist that is supported by tape, and subsequent light exposure and hard bake. The geometrical quality of the seal is usually quite poor. More serious is the disadvantage of the material itself, and particularly its invariable surface chemistry. To the author's knowledge, with the exception of plasma treatments[21], successful surface modifications of photo resist has not been carried out, The choice of substrates is very limited since the resists are optimized for silicon materials. Therefore, little is gained by forming walls and ceilings with polymers since the brittle and expensive base limits the size and utility of the device.

3.2.3. Traditional Surface Micromachining of Silicon and Glass

Traditional surface micromachining has its origins in the techniques developed for the IC industry to produce semiconductor circuits from silicon and other semiconducting materials. Surface micromachining, in a broad sense, is a well accepted, thoroughly researched multibillion dollar industry. It is ubiquitous at universities and companies, with a broadly available machine park. Currently, silicon and glass micromachining is still used extensively for the fabrication of specialized microfluidic devices at many institutes and universities due to unprecedented dimensional control and high precision.

Fabrication procedure for micromachining of silicon and glass

The traditional surface micromachining starts with the application of a protective organic layer, usually applied via spin coating. After standard procedural steps, such as pre-baking, photolithography is used to produce organic patterns on the silicon surface. After removal of non-crosslinked material, the surface is etched, and the material in unprotected portions is removed. Precise control of etchant, temperature and exposure time yields good etch depth control, see Figure 4. In Figure 4 **a)** a spin coated layer is exposed to light and non-crosslinked material is removed, resulting in a pattern that protects portions of the surface. The surface is etched in a bath, and unprotected regions of the substrate are slowly removed via a chemical reaction Figure 4 **b)**. In Figure 4 **c)** the finished permanent pattern is developed through removal of the protective organic layer with special resist solvents. These steps are repeated to construct layered features. To produce finished devices two to several substrates are bonded together and connections are machined through the substrate.

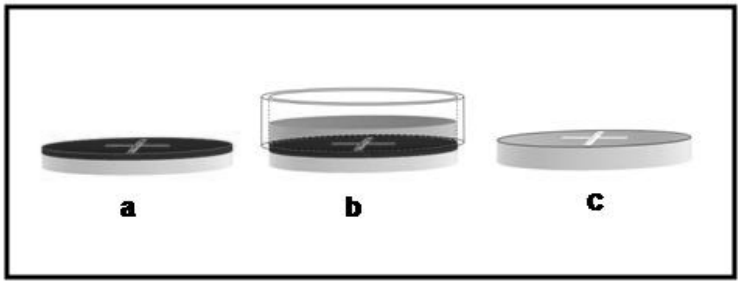

Figure 4 Traditional micromachining via spin coating and surface etching of Silicon or glass.

Advantages of micromachining of silicon and glass

Primarily, micromachining of Si-substrates is well known and mastered, yields precise devices and has well established surface modification techniques, such as plasma deposition.[6] Furthermore, series production of large quantities of identical devices is easily realized since the automation level for surface micromachining is high. Thus, millions of devices are produced at a few dollars per piece.

Apart from being well known, the level of precision, with incorporation of moveable parts, is simply unparalleled in the microfluidics field. Furthermore, many devices need electronic control circuits and sensors on-chip, which is possible to fabricate on the same die. To date, this has been difficult to achieve due to complex fabrication schemes with varying process conditions for the fluidics and the electronics. While this may be possible in the future, it is unlikely to be an inexpensive and fast process.

Disadvantages of micromachining of silicon and glass

Many of the disadvantages of silicon and glass based devices come from the fact that each device takes a long time to produce, with typical turnaround time of 3 to 9 months. For devices such as the one shown in Figure 2, microassembly protocols are extensive, very time consuming and therefore expensive.

Apart from cost and time consumption, other disadvantages are brittleness and materials invariability. Also, it is difficult to etch deep channels, i.e. more than a few tens of μms. This makes it very cumbersome to fabricate directly interfaces for interaction with macroscopic auxiliary equipment. Thus, devices need to be packaged for protection and interfacing, which adds cost and complexity.

3.3. Polymeric Microfluidic Devices

While fabrication techniques for silicon and glass microfluidic devices are constantly improving, the present research and commercialization focus has shifted to microdevices made entirely from polymeric materials. The main benefits of polymeric microdevices are low cost and durability, which suit field use and point of care diagnostic applications. The availability of numerous mechanical and chemical properties achievable based on simple chemical changes in the polymer formulations are also important advantages. Since each device requires substantial resources to develop and produce, efforts have been made to shorten optimization time through the use of rapid prototyping techniques, where device geometries are quickly evaluated. So far, the most promising techniques for fabrication of polymeric microdevices are silicon rubber (poly(dimethyl siloxane), PDMS) replication techniques such as soft lithography, [22] thermoplastic replication methods such as hot embossing and microinjection molding, and Microfluidic Tectonics.[23] Below, common techniques for polymeric microfluidic device fabrication are presented and the advantages and drawbacks are discussed.

3.4. Microfabrication Techniques for Thermoplastic Polymers

The most mature polymeric microfabrication technologies are various techniques of shaping thermoplastic polymers. As in the case for silicon and glass devices, this is largely due to tradition (machine availability, know-how, materials availability etc.), where macroscopic fabrication has been available for many decades.

3.4.1. Thermoplastic vs. Thermoset Polymeric Microfluidic Devices

The processing differs significantly from thermoset polymer microfabrication since the substrates are thermoplastic (except in reaction injection molding, RIM). Thus if the substrates are heated above the glass transition temperature, *Tg*, they become rubbery, or even liquid, and can be shaped against a template.

The final polymer properties differ between microfluidic devices fabricated from thermoplastic and thermoset materials since thermoplastic polymers already have attained a high molecular weight, while thermoset polymers are crosslinked networks formed from low molecular weight components. Thus, shaping of thermoplastic materials can be viewed as simply rearranging polymeric chains into the desired shape. Once such devices are produced, they can be shaped again by ambient factors such as heat (unlikely) and solvents. No bond breaking is necessary for these rearrangements, making devices more susceptible to damage, or more likely, imposes severe restrictions in their use.

Thermoset polymers, on the other hand, can not be macroscopically reshaped without breaking covalent bonds. Thus shape distortions are reversible, though it would be wrong to assume that they are unaffected by solvents etc. Furthermore, the shrinkage usually

associated with covalent bond formation during polymerization will leave residual stresses in the devices, risking brittleness and warping.

3.4.2. Hot Embossing

Hot embossing is a technique for the replication of patterns in thermoplastic sheets using a boss, which is a tool that has a permanent pattern on the side that faces the substrate. The technique is conceptually quite simple, and involves heating the boss and the work piece slightly above *Tg* of the thermoplastic work piece, pressing the boss into the material with a preset force, cooling the assembly below *Tg* and releasing the structure once it has regained its glassy, or semi-crystalline, state. In this manner, single layers with shallow patterns are easily fabricated. To fabricate enclosed channels, bonding of thermoplastic layers with heat, tone (glue) or other techniques are necessary.

Advantages of hot embossing

The main advantage of hot embossing is the size range that is afforded. Very advanced techniques for boss fabrication exist, which enables even nanometer size scales (ken carter).[24,25] Also, hot embossing is substantially less costly than injection molding, where the high pressure necessitates specialized machinery with high clamping forces, see Section 3.4.3. The lower pressures allow for less durable molds, where even polymeric molds have been used for the replication of hundreds of devices without degradation.[26]

Disadvantages of hot embossing

The primary disadvantages of hot embossing are longer production times per device due to slower thermal cycling than for injection molding. Thus, mass scale fabrication of thick devices is more costly than in injection molding. Also, channels produced are usually shallow and chip to world connections are difficult to achieve. Undercut structures can not be produced, wherefore assembly of separately fabricated layers is necessary for enclosed structures etc.

3.4.3. Microinjection Molding

Microinjection molding is very similar to macro-scale injection molding, except that there are much higher demands on mold precision. Typically, a thermoplastic polymer is melted and injected under high pressure into a mold cavity. The mold is rapidly cooled below the *Tg* of the polymer, opened and the finished device is ejected.

Advantages of microinjection molding

Microinjection molding allows for rapid production of many devices due to very efficient thermal cycling. Once the molds are fabricated, mass produced devices are attained. Compared with hot embossing, more geometrical freedoms are enjoyed, and multilevel structures where channels have different depths are readily produced.

Disadvantages of microinjection molding

The main disadvantage is the cost of the mold itself. Typically a high quality mold costs in the vicinity of $50,000. This is alleviated by rapid mold production schemes, where less expensive prototype molds are produced at a fraction of this cost. Still, microinjection molding is never an inexpensive or rapid solution for device development via prototypes.

Similar to hot embossing, assembly of separate layers are required for the construction of closed microfluidic devices.

3.4.4. Thermoset Polymeric Microfluidic Fabrication Techniques

The following sections detail fabrication techniques that have been labeled, and occasionally used, as large scale fabrication methods. Thus, purely prototyping schemes, such as stereolithography[6] and two photon lithography[27], are not discussed.

3.4.5. Soft Lithography

Soft lithography is a collective term for techniques used to construct microstructures from poly(dimethyl siloxane), PDMS. The first description of PDMS use for microfluidic applications were by Stenberg *et al.*[28] and has been further developed over a decade by Whitesides *et al.*[22] at Harvard University. Soft Lithography has later been expanded by Quake *et al.*[12] at Caltech (currently Stanford) and others. The importance of Soft Lithography for the microfluidics community has been, and still is, very large. With its advent, it was possible to design and fabricate microfluidic devices in a couple of days, which should be compared to weeks and months using traditional micromachining techniques. The rapid turnaround time enabled prototyping schemes where a number of different designs were produced and evaluated in an iterative fashion, resulting in optimized end products. Today, soft lithography has matured to the extent that it is being used commercially to produce microfluidic devices by a number of companies, notably Fluidigm, San Francisco, CA (http://www.fluidigm.com) and Celectricon, Gothenburg, Sweden (http://www.cellectricon.se).

Soft lithography microfabrication

Typically, PDMS structures are formed from molding against a negative image of the desired structure. The mold can be fabricated in many different manners, and the ultimate choice is determined by the desired resolution and the number of replications that the mold must withstand. Thus, for short prototyping series molds are made from spin coating and photolithographic patterning while large series production molds are made from metals. A typical production process is schematically outlined in Figure 5. In **a)** a spin coated layer is exposed to light and non-crosslinked material is removed, resulting in a pattern that protects portions of the surface. A mold is produced by the application of walls that are placed on top of the relief patterned substrate, **b)**. In **c)**, PDMS precursor is poured into the mold, and in **d)** the finished device is released from the mold after thermal curing. In **e)**, connections are punched through the PDMS layer with needles or hole-punchers.

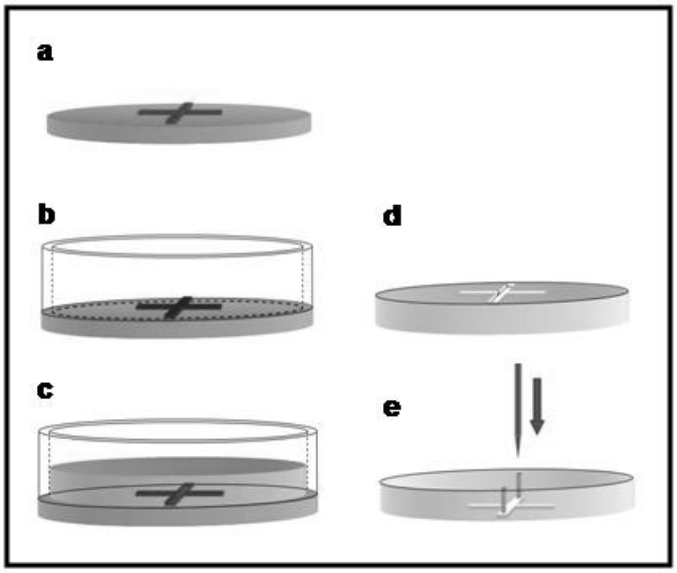

Figure 5 Fabrication scheme for Soft lithography.

Advantages of soft lithography

Soft lithography's main advantage, as has been previously mentioned, is the speed with which new devices can be produced. Furthermore, the required fabrication machines, such as mask alignment systems and spin coaters, are relatively inexpensive, i.e. less than $100,000.

The resulting devices have many attractive properties, such as chemical inertness, facile bonding, (both reversible and irreversible) to glass or other layers of PDMS and low modulus, which allows for efficient pumping schemes that are difficult to realize in more rigid materials.

Some researchers claim that the relative ease with which the surfaces are modified is advantageous compared to other materials, in particular the ease with which hydrophobic to hydrophilic transformations are achieved through oxygen plasma treatment. While this is a correct statement, it is slightly problematic due to the short lifetime of such modifications. Typically, plasma treated surfaces maintain their hydrophilicity only for a few days, which may be sufficient to conduct laboratory experiments and device verification, but is too short for commercial devices that need to have shelf lives in excess of weeks and even months. This is realized in the community and the issue has been addressed in a number of ways: larger molecules that attach to the surface increase the modification durability and network forming modification that significantly increase the surface stability, have been reported.[29]

Disadvantages of soft lithography

The main disadvantage of soft lithography is materials invariability. To date, PDMS is almost the sole material, although some olefinic rubbery polymers have been evaluated.[30] While PDMS has many attractive properties, it is incompatible with non-polar solvents. These solvents swell significantly the PDMS bulk, which risks blocking of channels, and even cause cross contamination of adjacent fluidic streams.

Furthermore, PDMS is usually thermally cured and patterned through material exclusion against a negative image mold. Normally, devices have connections through the layer, e.g. channels and reservoirs, and they must be manually fabricated with needles or hole-punchers in the finished device, with reduced precision and repeatability. For photolithographic applications at least one photopolymerizable PDMS precursor has been synthesized.[31]

3.4.6. Microfluidic Tectonics

Microfluidic tectonics is a direct polymer fabrication technique invented and developed by Moore and Beebe.[23] Superficially, this method has a close resemblance to CLiPP, see Chapter 5. Microfluidic tectonics will be presented in more detail than other fabrication techniques to aid CLiPP comparisons.

Microfluidic tectonics microfabrication

The polymer processing in microfluidic tectonics starts with the filling of a prefabricated "cassette" made from thermoplastic materials with a reactive monomer solution. This monomer is made reactive with photoinitiators and upon subsequent illumination by UV-light through a photomask that is placed on top of the cassette, transparent mask regions solidify. The photopatterned features are released by pushing solvent through openings in the cassette, see Figure 6. In **a)** monomer is filled in the cassette. In **b)** a mask is applied and the set up is exposed to UV-light. In **c)** solvent rinsing of the void is shown and the result is the finished device, **d)**, where the channel is indicated by a darker color.

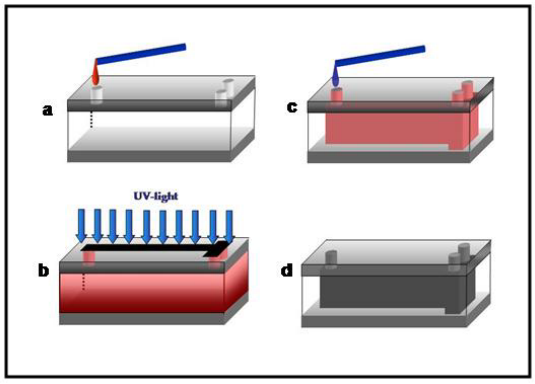

Figure 6 Processing steps in microfluidic tectonics

Methods for the fabrication of channel floors and ceilings from photopolymers have been described in papers and patents.[32] These involve immiscible, inert liquids that are flowed into the cassette and a denser monomer formulation is flowed underneath the inert layer. After the flow has stopped and a "quiescent state" has been reached, polymerization is effectuated. After rinsing, an arbitrarily thick polymer layer covers the bottom. Subsequently, the top portion is filled with a second monomer formulation, and a two layer structure is produced upon polymerization.

It should be noted that microfluidic tectonics does resemble a very basic method for device fabrication via photolithography. In this basic method, two glass slides are separated with shims or other structures with specific thicknesses and the gap between the slides are filled with a monomer solution. A mask is placed on top of the upper glass slide and upon polymerization through the mask a patterned layer with a predetermined thickness is produced. Obviously, microfluidic tectonics affords many advantages over this basic method since inlets and outlets, with facile access, are produced and the polymeric top and bottom are attached without further assembly.

Microfluidic tectonics materials

There is a very large array of materials available for photopatterning via microfluidic tectonics. The only demands are that they do not dissolve the thermoplastic cassette and that the have reasonable viscosities. Thus many different channel walls are easily produced.

Advantages of microfluidic tectonics

The main advantages of microfluidic tectonics are fabrication speed and materials versatility. Also, the thermoplastic sheets can be chosen for good optical transparency and mechanical robustness. The fully polymeric devices are also durable and easy to handle.

Disdvantages of microfluidic tectonics

Severe limitations in geometrical freedom are present in microfluidic tectonics. First, without resorting to very complex multilayer production schemes, only single layers are produced (not counting the thermoplastic top and bottom of the channels). The use of prefabricated cassettes results in predetermined access points, with different access geometries only available through the use of different cassettes. These are produced via injection molding or via other microfabrication techniques such as drilling and assembly of thermoplastic sheets. This may be both difficult and expensive in limited prototype test runs, and counteract the advantages of speed and low cost.

Also, the pattern is transferred through a thick plastic sheet which limits the resolution of channels and other structures. A minimum distance between features of 250 μm is claimed.[23]

Difficulties in producing hybrid devices, i.e. devices with silicon structures, electrical connections etc. are mainly due to limited access in the prefabricated cassettes. Despite these difficulties, such devices have been fabricated and presented.[33]

4. Photopolymerization

In the beginning of this chapter, fundamentals of photopolymerization via radical intermediates are presented. That part of the chapter is primarily for readers not familiar with photopolymerization processes and the typical characteristics of polymers produced in such processes. Later in the chapter, methods for experimental determination of polymerization kinetics are presented and applied to commonly used CLiPP monomers. The chapter serves as a background for discussions of the materials used in the CLiPP process, and the factors that determine patterning quality in CLiPP, which is the focus of Chapter 7.

4.1. Introduction

Photopolymerization has found an extensive industrial use as a versatile technology for coating various substrates. The technology presents several advantages such as low energy consumption, rapid processing, and reduced volatile organic compounds (VOC) since no solvents are necessary to ensure proper formulation viscosities. Due to the large use of industrial coatings, raw materials suppliers have ensured availability of many monomer types in high volume at low prices.

The fundamentals of polymerization are presented in the following section. Odian's *"Principles of polymerization"* is an excellent introductory text, and much of the material presented in the following sections is based thereupon. [34]

4.1.1. Radical Polymerizations

The radical polymerization process, i.e. the rapid addition of monomers to growing polymer chains, is typically conducted with carbon double bond containing monomers. However, there are exceptions such as radical ring opening polymerizations[35] and thiol-ene copolymerization.[36] Double bonds are well suited for radical polymerization since the radical attack is thermodynamically favored with very rapid reactions as a consequence.

4.1.2. Initiation

The radical polymerization process starts with a number of initiation events. Initiation is typically started by creation of radicals through the cleavage of covalent bonds. These radicals rapidly add to monomers and the chain polymerization process is started.

Only a small amount of the total monomer is consumed in the initiation step. Nevertheless, it has a large impact on polymerization speed and final polymer properties, e.g residual stress and mechanical strength. Under certain circumstances, a high radical production rate is necessary to counteract the consequences of extensive inhibition reactions, e.g. oxygen inhibition.

4.1.3. Propagation

Propagation is the rapid addition of monomers to growing polymer chains. The vast majority of the monomer is consumed in the propagation steps. In a typical monomer formulation, several thousands of monomers are added for each initiation event. Thus, there is a very large amplification of the incident light, a fact that is very important for patterning quality, see Section 7.2.

A second mode of propagation is shown by thiol-enes. Here, chain transfer events take place between each added monomer, which is an example of a step wise polymerization. This has large implications for network formation via cross linking, and results in lowered residual stress and lowered moduli.

4.1.4. Termination

Chains do not grow indefinitely and are typically terminated before all monomer is consumed as the reactivity of radicals is high. In the event of close proximity, two radicals combine to form a covalent bond, so called bimolecular termination. In most cases, termination is irreversible, although a notable exception, living radical photopolymerization (LRPP), is presented in Section 6.9. In fact, the termination reactions are so efficient that radical concentration often is relatively unchanged during photopolymerization. This so called steady state, with respect to radical concentration, is one of the cornerstones in treatments that lead to mathematical descriptions of polymerization kinetics. While other modes of termination have been described, bimolecular termination dominates in many systems.

In crosslinked systems, the mobility on a molecular level decreases rapidly as the polymer solidifies. It is therefore entirely possible to trap radicals in the network. In this case, the immediate environment sterically hinders approaches to the radical site sufficiently to prevent other radicals and even monomers from approaching. If this mode dominates, monomolecular termination kinetics is followed.

4.2. Kinetics

In this section, basic concepts and equations that govern and describe polymerization are introduced. The results are later used in the subsequent section that presents polymerization kinetics for typical CLiPP monomers.

4.2.1. Kinetic Equations and Assumptions

The basic kinetics developed for radical chain reactions take three separate steps into account: initiation, propagation and bimolecular termination, i.e. termination involving two growing chains, i.e. reaction (1) to (4) in Figure 7:

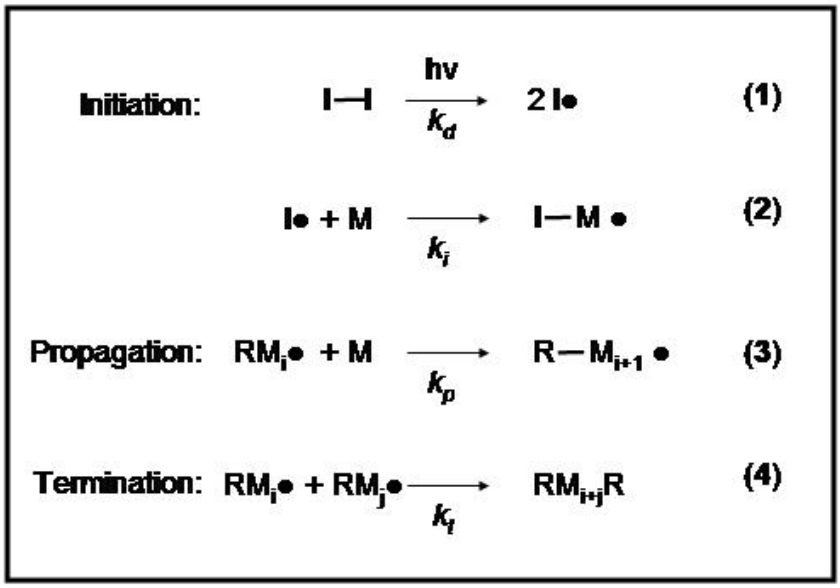

Figure 7 Generalized reaction schemes for chain-wise polymerization.

The equation governing the dependence of the rate of polymerization is: [34]

$$R_{Ptot} = k_p[M]\left(\frac{\Phi_i I_a}{k_t}\right)^{\alpha = 0.5} \qquad \text{Eq. 4.1}$$

In Eq. 4.1, R_{ptot} is the rate of monomer consumption, $\phi_i I_a$ is the rate of primary radical generated as a result of initiator cleavage, reaction (1) in Figure 7, and k_p and k_t are the rate constants for propagation and termination, respectively. The initiator efficiency, ϕ_i, is the fraction of radicals that starts a reaction after a photon has been absorbed. I_a is the number of photons absorbed by the initiator in a given period of time, commonly given in units of Es, photons/s. The coefficient α determines the relationship between the rate of initiation and the rate of polymerization. In the ideal case of solely bimolecular termination the coefficient α is 0.5, the value indicated in Eq. 4.1.

The following assumptions are made in the derivation of Eq. 4.1:

1) The initiation step is very fast. No reactions between the primary radicals and other radical species are taken into account, i.e. k_{tprim}, $k_{tpinit} << k_{ti}$. The allowed exception to this assumption is the reaction of radicals from the initiator that upon formation recombines within the solvent cage. This is reflected in the value of the initiator efficiency ϕ_i.
2) The steady state approximation is used, i.e. the radical concentration remains constant throughout the reaction.
3) The initiation step is assumed to consume only a small amount of monomer compared to the propagation. This assumption is justified if high molecular weight polymers are formed. An often-quoted limit for this is 100 monomer residues per initiating radical, with the error increasing for successively lower kinetic chain lengths.[37]
4) All polymer radicals (RMi● in reaction (3)) are considered equal in reactivity towards both propagation and termination regardless of size.

4.2.2. Kinetics in Monovinyl Systems

The kinetics in monovinyl systems sheds light on fundamental factors that also govern the crosslinked, monomer formulations typically used in photolithographic processes. Therefore, kinetics of different monovinyl monomer functionalities were extensively studied with Photo Differential Scanning Calorimetry (photo DSC, see Paper III for experimental details) and Photo Real Time Fourier Transform InfraRed spectroscopy (photo RTIR, see paper IV for experimental details).

Kinetics evaluations take on many different forms, depending on the level of information that is desired. In photolithographic processes, the dependence of polymerization rate on light intensity, α, is an important parameter. The numerical value of α is important for the elucidation of the basic mechanisms that dominate the polymerization of a particular monomer type. A value different from the ideal (α=0.5) in Eq. 4.1, depends on a deviation from the assumptions listed above: i) deviation from assumption 1 results in $\alpha < 0.5$;[3,4] ii) deviations from assumptions 2, 3, lead to $\alpha > 0.5$; and iii) deviation from assumption 4 is either reducing or increasing α (in the case of chain length dependent termination (CLDT) $\alpha < 0.5$ and in the case of chain length dependent propagation (CLDP) $\alpha > 0.5$).

It is shown in Paper III that Eq. 4.1 can be put in a different form that is more amenable to the determination of α from kinetic parameters determined via photo DSC and photo RTIR:

$$\frac{\ln[M_0]-\ln[M]+C}{t} = kI_a^{\alpha} \qquad \text{Eq. 4.2}$$

In Eq. 4.2, t is the reaction time, $[M_0]$ is the initial monomer concentration, [M] is the monomer concentration at polymerization time t, C is the integration constant, k is a lumped rate constant and I_a is the absorbed light intensity.

In the following sections, kinetics evaluations of monovinyl acrylates, methacrylates and vinyl ether maleates are presented. The instrumentation choice varies due to different time

resolutions in the photo RTIR and photo DSC set-ups used in this study. For acrylates, the sampling rate of the photo-RTIR set-up was insufficient to yield acceptable data. The photo DSC technique was therefore used for acrylates. For methacrylates, the very low polymerization rates at low light intensities lead to irreproducible results, and the photo RTIR set-up was used. The vinyl ether/maleate formulations were recorded with both photo DSC and photo RTIR.

Acrylate polymerization

Acrylate kinetics has been described thoroughly in the literature.[38,39] Nevertheless, experimental details are shown for two reasons; i) comparisons with other functional group kinetics are simplified by utilizing identical, or very similar, reaction conditions; and ii) the kinetics are known and serves as method validation. Experimental details and apparatus descriptions are found in Paper III. The development of cure over time recorded with photo DSC is shown for several light intensities in Figure 8.

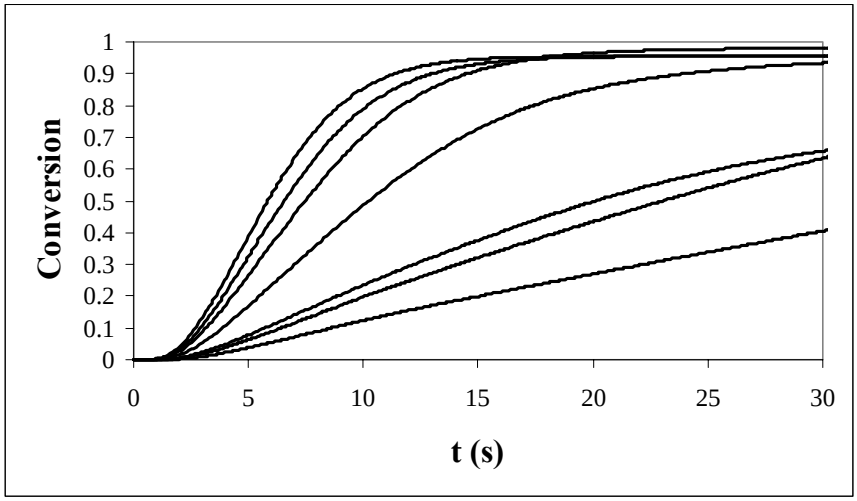

Figure 8 Conversion vs. time in dodecyl acrylate with 2% Irg 184. Intensities were 0.21, 0.49, 1.03, 3.09, 7.20, 10.95, 16.40 mW, respectively.

Starting at 1% conversion and continuing in increments of 0.5% the coefficient α is determined via Eq. 4.2, see Figure 9. The average value of α is approximately 0.48 (between conversions of 0.2 to 0.7), which is reasonably close to the expected value of 0.5, the difference not being statistically significant on a 90% confidence level.[40] Similar results have been reported previously by researchers,[41] and indicate that the aforementioned kinetic approximations are valid in this system.

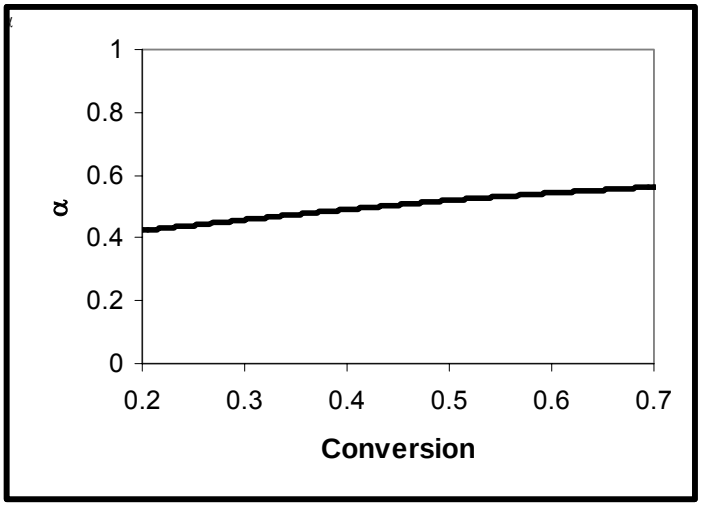

Figure 9 The coefficient α as a function of conversion in dodecyl acrylate with 2% Irg 184. The average value is ≈0.48.

Some features in the graph are somewhat surprising and need to be explained. A very clear trend in Figure 9 is the increase in α with conversion. This is contrary to the usually observed *decrease* in initiator efficiency with higher conversion in linear systems, and is therefore suggested to be an artifact. The cause is hypothesized to be an inability of the detectors to keep up with the rate of heat liberated during very fast polymerizations. Heat developed at low conversion is therefore recorded at a later stage in the polymerization process. This tends to make the slope larger at higher conversion (reflected in the increasing α). A further indication for this interpretation is that at higher intensity the peak exotherm occur at higher conversions (graph not shown). In the case of dodecyl acrylate ΔH_{max}(I=0.21 mW) is at 8% conversion and ΔH_{max}(I=16.40 mW) is at 36% conversion. This behavior can not be inferred from the elementary reaction steps and is likely an effect of cumulative heat transferred to the detectors.

Methacrylate polymerization

Contrary to acrylate polymerizations, methacrylate polymerizations described in the literature have been found to deviate from ideal kinetics. [42] The results presented in Figure 10 shows an average coefficient of 0.36, well below 0.5, the difference being significant on a 99% confidence level. This result is in accordance with previously published results.[43]

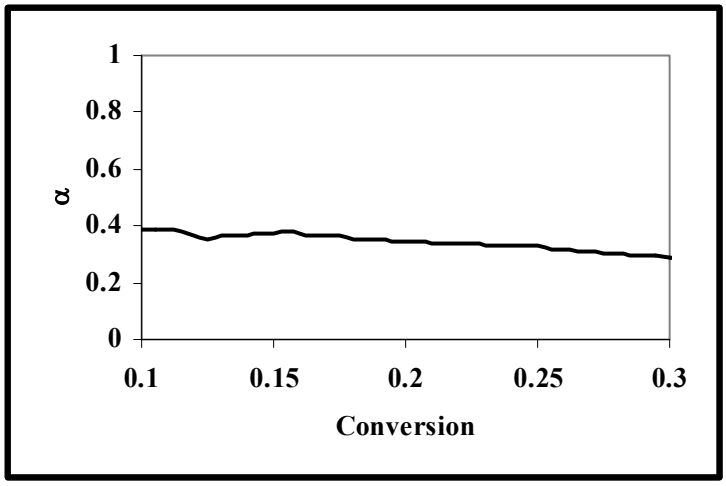

Figure 10 The coefficient, α, as a function of conversion in dodecyl methacrylate with 2% Irg 184, as determined with photo-RTIR. The average value is ≈0.36.

The deviation from the kinetics described by Eq. 4.1 has been attributed to chain length dependent termination, CLDT. [44,45] Chain length dependence is considered to originate from the decreasing diffusion rates of radical fragments with increasing molecular weights. Larger fragments will diffuse more slowly, reducing the probability of encountering another radical fragment for bimolecular termination. This has been shown with computer models, in which CLDT leads to $\alpha \approx 0.3$. [46]

Vinyl ether/maleates

The following sections are a compilation of Papers III and IV. In these papers several methods are utilized to gain insights into the factors that govern vinyl ether maleate polymerization. Polymerization kinetics is evaluated with photo-DSC (Paper III), photo-RTIR (Paper IV) and radical structures are determined with EPR (Paper IV). For all experimental details, see the relevant paper.

Several studies have concluded that vinyl ether/maleate formulations polymerize via an alternating mechanism.[47,48] The vinyl ether functional group is electronegative,[49] preventing radical homopolymerization while maleate homopolymerization is slow due to steric hindrance.[50] When stoichiometrically mixed and in the presence of a radical initiator, maleates and vinyl ethers polymerize rapidly.[51] Due to this crosspropagation, the reaction rate in these systems is controlled by specific monomer characteristics, such as side groups and abstraction sites, of both monomers.

In this study three vinyl ether monomers have been used, see Figure 11: (**1**) 1,1-dimethyl hexyl vinyl ether (BASF, Ludwigshafen, Germany), MHVE has no easily abstractable hydrogens while (**2**), 2-ethyl hexyl vinyl ether (Aldrich Chemical Co., Milwaukee, WI) has two readily abstractable α-hydrogens[52] and one abstractable tertiary hydrogen. To elucidate the importance of tertiary hydrogen sites dodecyl vinyl ether DDVE (**3**) was also utilized. In this monomer, there are readily abstractable hydrogens, but no tertiary

hydrogen site. In the formulations, diethyl maleate (Aldrich), DEMA (**4**), was used as the co-monomer. In all formulations, 2% (w/w) of the photoinitiator 1-hydroxy cyclohexyl phenyl ketone (tradename Irgacure 184 (Ciba, Tarrytown, NY), (**5**) was employed**.** While EHVE and MHVE are identical in most respects, some monomer differences affect the polymerization kinetics. Firstly, the polymer chains forming during the polymerization of MHVE/DEMA are stiffer than in EHVE/DEMA due to steric interference between the α-methyls and the carbon-carbon backbone. This is likely to cause an increased viscosity at similar conversion levels, which in turn affects termination reactions. Secondly, the absence of abstraction sites in MHVE/DEMA minimizes both chain transfer reactions and subsequent reinitiation and termination reactions that are possible in the EHVE/DEMA formulation. DDVE has a higher molecular weight than MHVE and DEMA, leading to lower monomer concentrations in the DDVE sample.

The vinyl ether/maleate monomer ratio was kept constant at 1/1 on a molar basis since the polymerization is alternating.

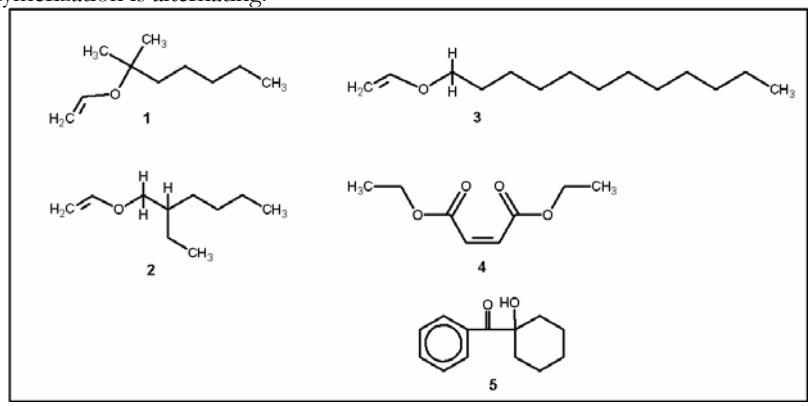

Figure 11 Chemical formulae of the compounds used in the study.

The presence of abstractable hydrogens dramatically affects the rate of polymerization, R_p. As seen in Figure 12, both the EHVE/DEMA and DDVE/DEMA formulation exhibits a significantly slower polymerization than MHVE/DEMA in a photo DSC study.

Figure 12 shows normalized vinyl ether/maleate copolymerizations (photo DSC) of MHVE/DEMA, EHVE/DEMA and DDVE/DEMA at two different light intensities. The black lines are the conversion vs. time traces that corresponds to a high light intensity and the gray traces correspond to a low light intensity. The bold black trace in **a)** represents MHVE/DEMA polymerization at 14mW/cm^2 and the bold gray trace represents the MHVE/DEMA polymerization at 7 mW/cm^2. The black trace **b)** represents DDVE/DEMA at 16mW/cm^2 and gray DDVE/DEMA at 7mW/cm^2. The thin black trace in **c)** is EHVE/DEMA at 14mW/cm^2 and thin gray trace is EHVE/DEMA at 7mW/cm^2

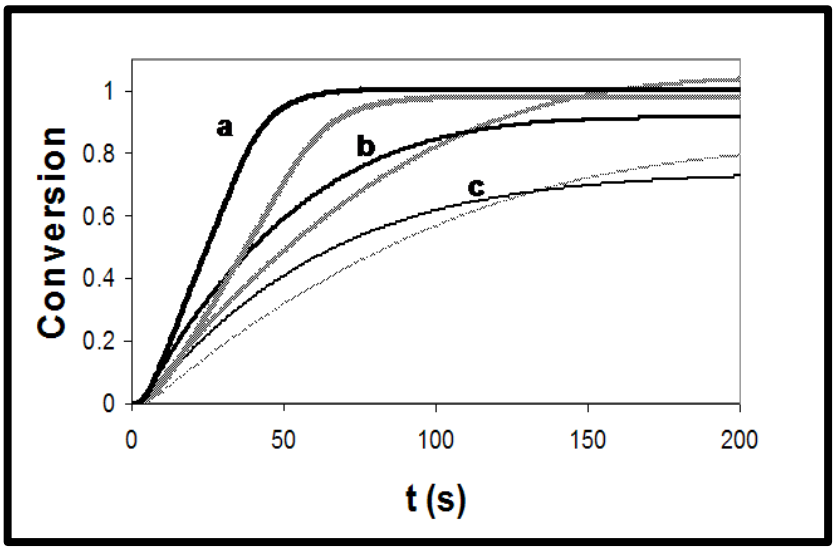

Figure 12 Normalized Vinyl Ether/DEMA copolymerizations (data recorded with Photo-DSC and converted to conversion vs. time).

These results indicate that the hydrogen abstraction process is efficient. This is coupled with a slow subsequent reinitiation reaction or very high termination rates of the radicals that result from the abstractionprocess. To elucidate which effect dominates, the structure and the nature of the radicals that result from an abstraction reaction need to be considered.

Radical structure in vinyl ether/maleate polymerizations

There are two techniques suitable for the elucidation of the radical structures in the vinyl ether/maleate systems studied: i) the direct method of Electron Paramagnetic Resonance spectroscopy (EPR); and ii) the indirect method of photo RTIR.

In EPR, the radicals absorb electromagnetic radiation with energies that are directly linked to the local environment around the radical. [53] Through analysis of EPR spectra, the structure of the radical is determined, see Paper IV for a more detailed description of reaction conditions and interpretation.

EPR studies on MHVE/DEMA and EHVE/DEMA show the different radicals present during polymerization, see Figures 13 and 14. In both graphs, a homopolymerization spectra obtained with DEMA is included. The maleate radical has a large three peak spectrum centered around 3350 G, indicated by the bold black trace.

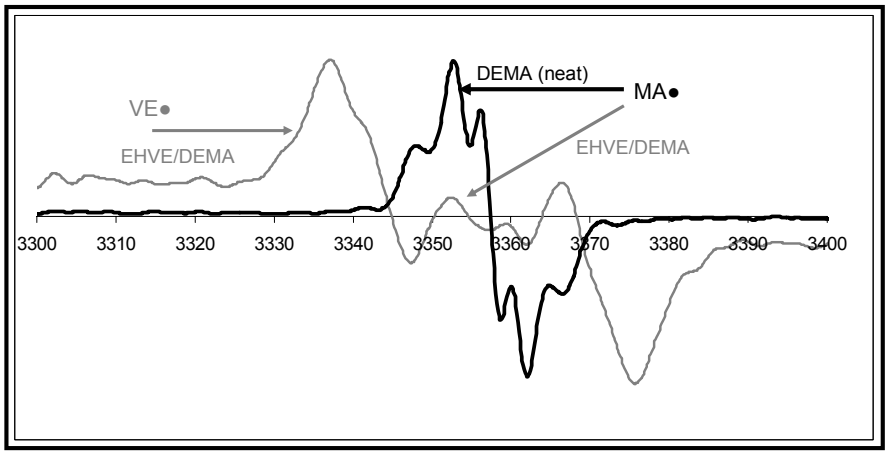

Figure 13 EPR spectra of EHVE/DEMA polymerization. Black line is DEMA polymerized neat and gray is EHVE/DEMA polymerized under the same conditions.

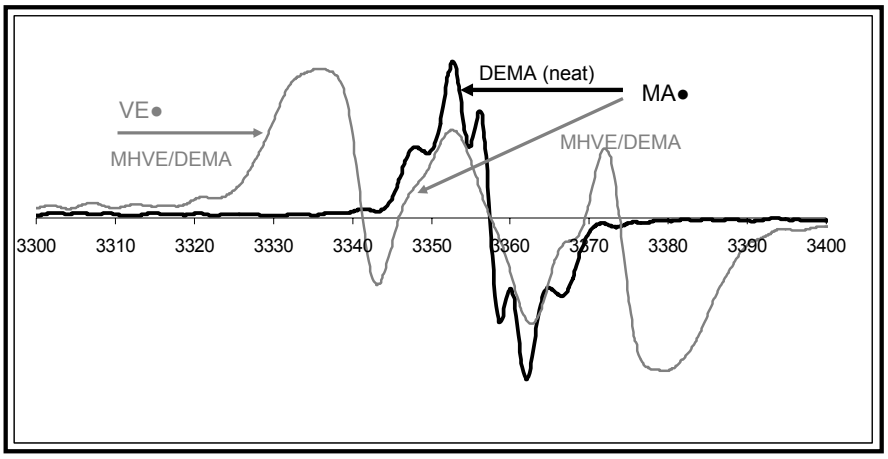

Figure 14 EPR spectra of MHVE/DEMA polymerization. Black line is DEMA polymerized neat and gray is MHVE/DEMA polymerized under the same conditions.

Comparing the above figures shows clearly that the maleate radical peak almost disappears during the EHVE/DEMA polymerization. This is clearly supporting that the maleate radical abstracts a hydrogen from the vinyl ether, creating a vinyloxy like radical, see Figure 15.

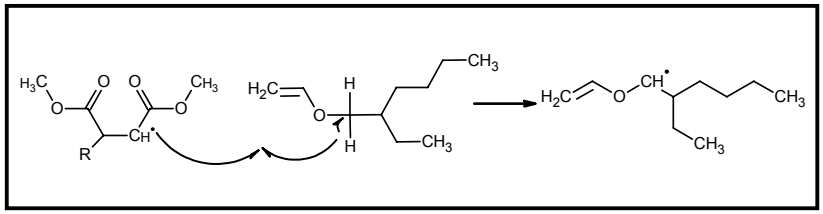

Figure 15 Likely structure of vinyloxy-like radicals in EHVE resulting from an abstraction event.

It is speculated that the abstracted radical has similar properties to the propagating vinyloxy radical. If this is correct, there should be an increase in maleate consumption in the EHVE/DEMA formulation. To address this, photo RTIR studies were conducted, for experimental details see Paper IV.

IR-spectroscopy is a method that uses electromagnetic radiation to detect molecular bonds. Each bond has a certain absorption energy associated with it. Frequency, or wavelength, scans result in spectra that identify the presence of certain chemical groups, both qualitatively and quantitatively. This is used in polymerization studies to assess the disappearance of reactive groups during the reaction.

Shown in Figure 16 are two sections of the continuous real time measurements of mid IR absorbance between 4000 cm^{-1} and 750 cm^{-1}. The top spectrum is recorded before illumination and the lowest intensity spectrum is recorded at the end of the illumination period. In **(a),** the combination vinyl area centered at 1640 cm^{-1} for MHVE/DEMA is shown. **(b)** Shows the maleate area centered at 1404 cm^{-1} for MHVE/DEMA. **(c)** corresponds to the combination vinyl area centered at 1640 cm^{-1} for EHVE/DEMA. **(d)** is the maleate area centered at 1404 cm^{-1} for EHVE/DEMA.

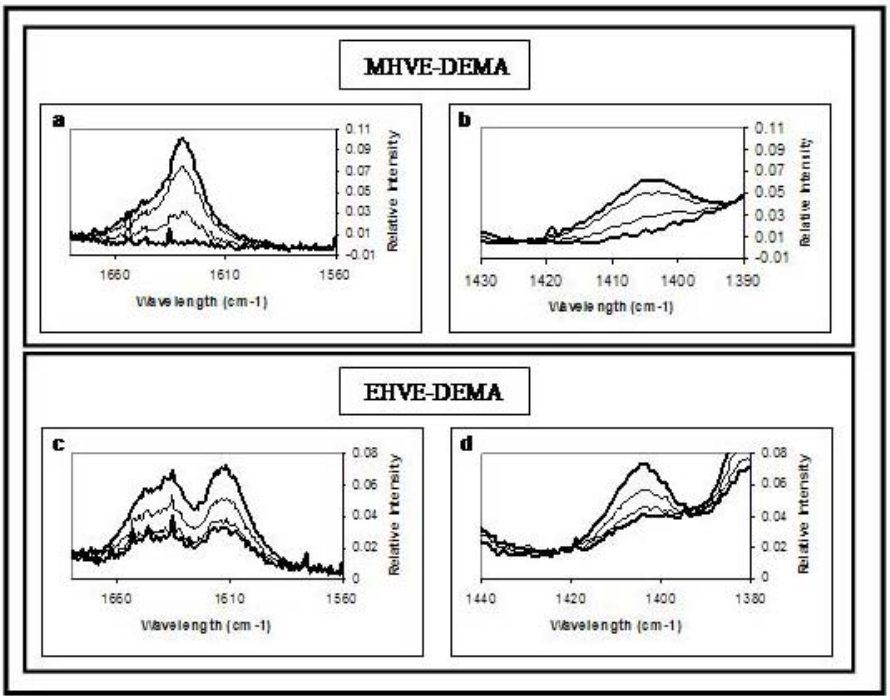

Figure 16 Time resolved spectra for the photo RTIR kinetics study of vinyl- ether DEMA co-polymerizations, MHVE/DEMA and EHVE/DEMA, respectively.

It is seen in Figure 16 that EHVE-DEMA exhibits a lower level of conversion than MHVE-DEMA. Also, comparing the relations between the spectra **a** and **b** to **c** and **d** there appears to be a difference in the relative monomer consumption.

A conversion as a function of time plot of both functional groups in the vinyl ether/maleate mixtures shows this more clearly, see Figure 17. In both graphs, the thicker line represents the maleate conversion and the thinner represents the combined vinyl conversion, i.e. both vinyl ether and maleate functionalities.

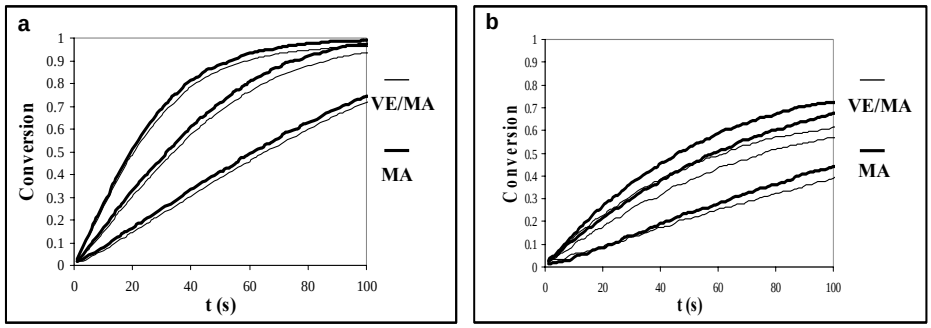

Figure 17 Comparison of individual monomer conversion at three different light intensisites in ***(a)*** *MHVE/DEMA and* ***(b)*** *EHVE/DEMA.*

The relative consumption of the two monomers is determined by examining the specific conversion profiles of the two IR bands. In Figure 17 **a)**, the maleate appears to have higher reaction rates than the vinyl ether. However, the differences are at all times lower than 5%, which is within the margin of error for RTIR measurements. Examining Figure 16 **b)**, it is apparent that a straight baseline will underestimate the amount of maleates in the mixture, since the final spectra will yield a conversion >1. This underestimation of $[MA]_0$, i.e. the initial maleate concentration, is the likely explanation for the apparent maleate polymerization rate.

In Figure 17 **(b)**, the EHVE/DEMA system, the relative difference between the maleate and combined vinyl conversion is much larger. Because of the alternating nature of the polymerization process, the increased consumption of one of the co-monomers will decrease both the overall rate of polymerization and maximum conversion.

α as a function of conversion in vinyl ether/maleates

Further insights into the polymerization mechanism are gained by evaluating the coefficient α as a function of conversion for the two systems, see Figure 18.

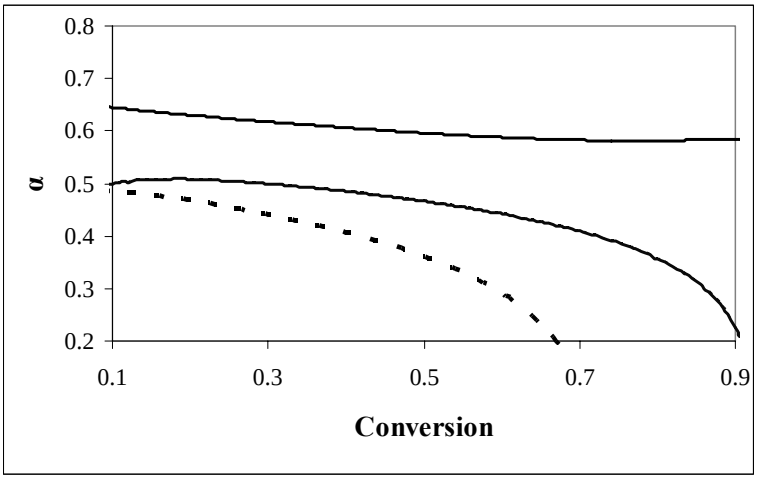

Figure 18 The coefficient α as a function of conversion. The upper solid line depicts MHVE/DEMA, the middle solid line is DDVE/DEMA and the lower dotted line is EHVE/DEMA.

The differences between the systems EHVE/DEMA and DDVE/DEMA, both systems with abstractable hydrogens, compared with MHVE/DEMA are apparent in Figure 18. The DDVE/DEMA and EHVE/DEMA systems initially do not differ significantly from the square root value at low conversions, with $\alpha=0.49 \pm 0.02$ and $\alpha= 0.45\pm0.03$ between conversions of 0.1 to 0.4, respectively. The MHVE/DEMA system, on the other hand, exhibits an α trace significantly above the square root value, with an average $\alpha=0.63 \pm0.02$ between conversions of 0.1 to 0.4. For EHVE/DEMA and DDVE/DEMA, α values are dramatically reduced at higher conversions, while those of MHVE/DEMA remains relatively unchanged.

The most likely explanation for the deviation from the square root behavior in MHVE/DEMA is Chain Length Dependent Propagation (CLDP), i.e. assumption 4 is false.

CLDP favors high initiation rates since shorter polymer radicals have higher k_p than longer ones. Therefore, R_p has a higher dependency on R_i than would be expected in a system where k_p is independent of the size of the propagating polymeric chain.

A description of DDVE/DEMA and EHVE/DEMA polymerization is more complex than is the case for MHVE/DEMA due to the added chain transfer reactions. Qualitatively, extensive chain transfer and subsequent slow reinitiation favors either unimolecular termination, i.e. a higher α, or reactions with initiator radicals, (primary radical termination), i.e. a lower α. The data is insufficient to dismiss either effect, but the lowered α compared to MHVE/DEMA supports an increase in primary radical termination.

The drop in α at conversions above 0.5 for EHVE/DEMA and DDVE/DEMA is likely linked to slow polymerization in combination with primary radical termination. At high light intensity and long exposure time, the initiator concentration is sufficiently lowered to impact R_i. This in turn affects R_p and, hence, α is lowered.

4.3. Oxygen Inhibition

Radical polymerizations are typically sensitive to oxygen inhibition. In its ground state, oxygen behaves like a biradical due to one electron pair that located in an antibonding orbital. Thus, oxygen reacts very rapidly with carbon based radicals, forming a covalent bond and an oxygen based peroxy radical, in the process. The peroxy radical is not reactive to carbon double bonds, but can terminate a second carbon radical.

Most lacquer formulations that have not been purged by nitrogen or other inert gases contain 2-3 mM oxygen.[54] For any polymerization to occur, radicals produced during the photoinitiation must consume all oxygen. This phenomenon is responsible for a short inhibition period always noticed during polymerization in systems exposed to air.

Dissolved oxygen does not create large problems in most bulk photopolymerizations because of the high radical production rates. It is only in systems open to the atmosphere that the oxygen inhibition effect is noticeable, due to the large proportion of oxygen in air (21%) and replenishment of consumed oxygen by the rapid diffusion of gas molecules.

The main effect of oxygen inhibition in systems open to the atmosphere is a thin uncured, or partially cured, top layer. Depending on specific curing conditions, this layer has varying thicknesses, typically in the range of a few to tens of μms.

4.4. Crosslinking

To obtain durable and chemically resistant structures, crosslinking reactions are used to generate infinite polymer networks. Crosslinked polymers are distinguished by their ability to resist creep (deformation due to shear forces), high chemical resistance, high temperature resistance and high impact resistance. Crosslinks are typically formed by the use of multifunctional monomers and oligomers.

4.4.1. Photopolymerization Phenomena in Multivinyl Formulations

A number of factors affect the performance of the final polymer. Primary among these are the degree of crosslinking in the polymer and the residual stress present in the film, i.e. overall magnitude and spatial distribution. The spatial distribution of the residual stress depends on the polymerization history and is closely linked to inhomogeneous cure.

Inhomogeneous cure

In a system that polymerizes by light, inhomogeneous film cure is caused by attenuation of the light as it passes through the film. The top portion of the film receives more light and the rate of polymerization is much higher than at the bottom portion of the film. Inhomogeneous cure lead to polymeric material properties variations through the film. Optical and mechanical properties are primarily affected, where the top layer has higher refractive index and a higher level of residual stress compared to the bottom layer.

Autoacceleration

Autoacceleration is a very common phenomenon in network forming polymerizations. Typically, when the viscosity has reached a threshold, bimolecular termination is suppressed by mobility restrictions, while polymerization is less obstructed due to the

small size of monomers. Thus a sharp increase in R_p is experienced when the gel point is reached. The starting point for autoacceleration depends on many factors, e.g. polymerization mechanism and crosslinking density.

Stress development

The overall residual stress level is important in thick films, since high levels of residual stress risk film cracking and delamination from underlying substrates.

The residual stresses measured for UV-cured multifunctional vinyl monomers are substantial, with reported values between 2-39 MPa.[55], The residual stresses may lead to lowered impact mechanical strength in the final polymer film.

The effect of stress on the final mechanical properties of the polymer is not only dependent on the overall magnitude, but also the manner in which stress is spatially distributed.[56] In industrially cured coatings, there is normally a conversion gradient in the film, i.e. non-uniform cure, due to specific polymerization process parameters such as the presence of short wavelength light, which is absorbed in the upper portion of the film, high light intensities and high initiator loadings.[57] The overall effect of these polymerization parameters is a high radical production rate in the upper layers of the polymer film during polymerization, which leads to an uneven stress distribution.

In most commercial polymer systems, uniaxial residual stress is of minor importance since the E-modulus of the polymer film is sufficiently high to withstand the forces without cracking or crazing. However, there are chemical and process specific factors that lower the *Tg* and modulus to such an extent that macroscopic failure of the films occur at very low impact energies, see Paper III.

5. Contact Liquid Photolithographic Polymerization, CLiPP

This chapter introduces the Contact Liquid Photolitographic Polymerization (CLiPP) process and its inherent capabilities and limitations. Comparisons between CLiPP and the fabrication methods described in Chapter 2 are made. A large portion of the chapter is dedicated to instrumentation; its development and features that are used to solve CLiPP specific-challenges. Different techniques for the fabrication of multilayer CLiPP structures are described. The fabrication techniques have also been described in Papers I, II and V, but some new information regarding recent developments are included.

5.1. Why a New Microfabrication Method?

As was seen in Chapter 2, microfabrication alternatives abound. Surely, arbitrary combinations of these methods should make it possible to meet all microfluidics challenges? In a broad sense this question can be answered affirmatively; all challenges can be met if each difficulty is addressed by the method best suited to solve it. Different parts thus fabricated are subsequently microassembled to form the finished device.

However, microassembly is not simple, and forming leak-free joints between different materials is even more challenging. Furthermore, few research groups have access to all the necessary equipment. Surely, large collaborations are established and advanced hybrid devices are produced, though it is widely realized that the use of too many different techniques does not represent an optimal design and fabrication process.

Much would be gained by the advent of a method that combines materials flexibility for facile, seamless integration of different substructures, simple fabrication of small-scale features, such as internal device channels and fabrication of large-scale macroscopic interface structures. Unfortunately, no such method yet exists. Fulfilling these stringent demands, while paying attention to all the previously mentioned microfabrication challenges, see Section 2.1.3, is very difficult. Nevertheless, it was with these requirements in mind that our group at the University of Colorado set out to design a novel microfabrication method.

5.2. The Advent of CLiPP

The beginnings of CLiPP can be traced back to studies on living radical polymerizations for facile surface modification via grafting, performed in Christopher Bowman's and Kristi Anseth's groups by Ning Luo and John Hutchison at the University of Colorado.[58] In this work, methacrylate monomers were polymerized in the presence of a reactive moiety called a photoiniferter*, see Section 6.9 for details of photoiniferter precursor reactions, see Figure 19. The photoiniferter enables subsequent reactions upon illumination, In

* Actually, the photoiniferter used is a precursor. It is only after cleavage and subsequent capping of a radical that it becomes an iniferter. Hereafter in the text it will be called an iniferter or photoiniferter, though it is not a strictly correct term.

Figure 19 **a)** a schematic of the living radical photopolymerization grafting method is shown. Initiation of an iniferter-containing surface in the presence of pure monovinyl monomer yields polymer grafted to the surface is shown. In **b),** a hydrophilic monomer grafted to the surface of a device and stained with an aqueous dye.

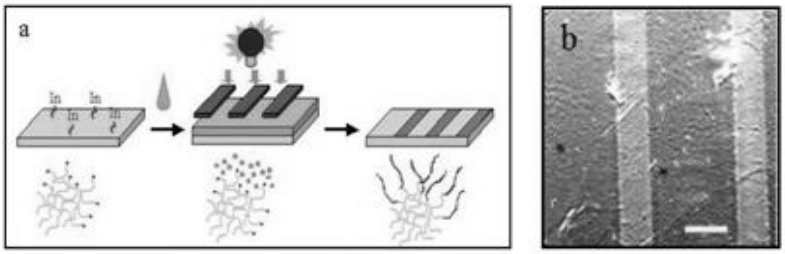

Figure 19 Surface grafting via photoiniferter precursors. (Schematic and Picture by Brian Hutchison)

It was realized that polymers containing photoiniferter precursors is an excellent choice for fully polymeric microdevices, but there was no method available for controlled fabrication of polymeric layers. Spin coating was considered, but developing monomer formulations with defect free surfaces, e.g. level and pinhole free, was a major obstacle and would limit the materials freedom.

The second important development of the CLiPP technology came a couple of years later, when, simply, a drop of monomer was contacted with a photomask in a standard mask alignment set up (unmodified OAI 200 mask alignment system). After UV exposure through the mask, the resulting polymer had a level top surface and well defined patterns. After some thought, it was apparent that the hereby established principle, i.e. a reactive monomer formulation in contact with a photomask, could be utilized in a specially designed mask alignment system to fabricate controlled layers without having to develop any particular process enhancing features via solvent and additive additions.

5.3. CLIPP Fundamentals

The three main features of CLiPP are:

i) liquid monomers polymerized in contact with the photo mask,
ii) sacrificial materials that are readily removed once the device is finished
iii) the use of living radical processes.

Having liquid precursors polymerized in contact with the mask has many important advantages. It provides for a convenient way to control layer thickness as well as surface geometries. It also enables better feature reproduction since the thin layer of air that is usually present between the mask and photoresist is eliminated, i.e. light refraction is limited. Furthermore, contact with a mask counters problems associated with atmospheric oxygen inhibition and eliminates the need for flow controlling additives and solvents in the formulation since leveling is provided by the mask. Independence of viscosity and flow properties provides for almost unlimited formulation choices. This ability opens the microfluidics field to devices constructed from polymers with a wide range of materials properties. Rubbery, glassy, hydrophilic and hydrophobic polymers are easily accessible, addressing different needs in optimized devices.

Sacrificial materials are a mainstay in the IC industry, and CLiPP utilizes them in a similar manner. With the aid of sacrificial materials, previously fabricated channels and voids are blocked, and subsequent layers are polymerized independently of the patterning of previous layers. In this manner, undercut structures are easily fabricated, and complex 3-D structures, that use optimally the allotted space, are accessible.

The living radical process ensures that polymerized surfaces, i.e. finished layers, are still reactive upon subsequent exposure to UV-light. Thus, layers that are fabricated on top of previously polymerized layers are covalently bonded and form monolithic structures. The mechanism is sufficiently general to allow for covalent bonding between monomers with different functionalities, as long as they react via radical intermediaries. Furthermore, surface initiated reactions are used to provide very thin layers of polymer that serve as surface modifiers without affecting polymeric bulk properties. This is a very useful feature for bio detection and bio compatibility.

5.4. Tooling Evolution

The tooling for CLiPP has undergone a rapid evolution, and it is of interest to account for these developments for two reasons; 1) in this thesis, each presented device has been fabricated with one, or more, of the available tooling set ups; 2) the development of the tooling shows how features are improved while the basic concept remains unchanged; and 3) the first tooling set shows how the CLiPP process can be evaluated through the use of very inexpensive equipment, provided that there is access to a mask alignment system. The following sections may be somewhat confusing since the fabrication sequence has not been presented in detail. It is suggested that 5.5 is read cursively before reading the tooling section.

5.4.1. First Tooling Set

The first tooling set up was manufactured in-house at the University of Colorado, from drawings provided by the author. The tooling set was not intended for stand alone use, but in combination with a mask alignment system, or at the very least a collimated light source. The basic tasks that the prototype tooling needed to accomplish were; i) provide a way to control the distance between the mask and the substrate; and ii) provide a manner for retaining liquid monomer on the substrate and prevent it from overflowing into the mask alignment system. The solution consists of a 2.54 cm x 2.54 cm stainless steel box, and stainless steel shims that fit snugly, see Figure 20. The operation of this tooling set-up follows the description in Section 5.5.2, with the difference that the distance between substrate and mask is controlled by the removal of shims instead of a moveable chuck..

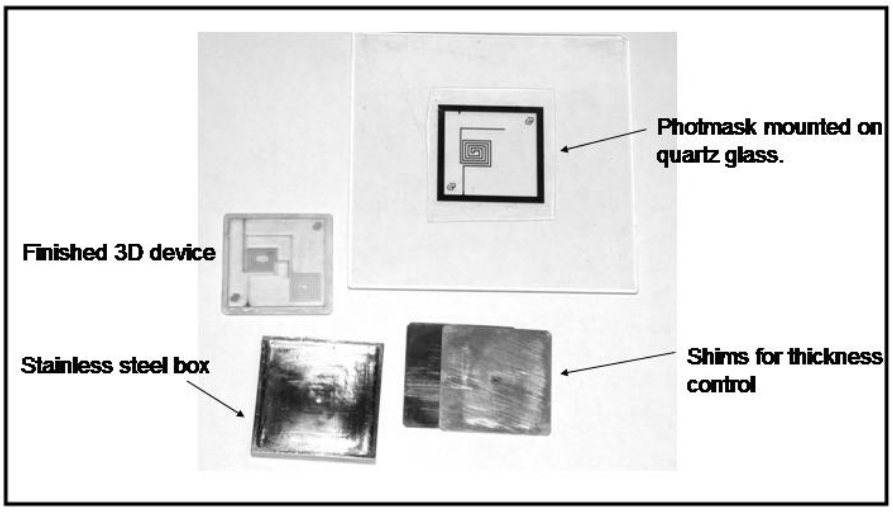

Figure 20 The first set of CLiPP tools

The specific characteristics of the tooling system used with an unmodified OAI 200 mask alignment system are shown in Table 1.

Table 1 Characteristic features of the first tooling set, all units in μm.

Minimum feature resolution	Alignment accuracy*	Layer thickness accuracy†	Maximum‡/minimum thickness
20	**±50**	**±50**	**1000 /100**

* Determined by microscopy inspection
† Determined by profilometry
‡ Total device thickness

Evaluation of the first tooling set

It was found that the major problem with this initial tooling concept was device tapering, i.e. the mask is at a small angle to the substrate. Typically, it was possible to control the tapering to ± 50 μm, which was adequate for proof of concept devices. However, for functional devices produced in small series scale, which is important for functionality evaluation, better control of the geometry was needed. The experiences from the first tooling set was incorporated in an in-house built modification of the original tooling set of an OAI 200 mask alignment system.

5.4.2. Second Tooling Set

As the basis for the experimental set-up used for the majority of the devices shown in this thesis, a Hybralign 200 mask alignment system (OAI, Milpitas, CA) with a 7.62 cm diameter UV light source (Oriel Instruments, Stratford, CT) is used. Shown in Figure 1 is a drawing of an in-house designed polymerization chamber. The system provides a 5.1x5.1 cm polymerization area and bottom plate that is vertically moveable 5 mm. Micromanipulators for alignment in the x-y plane were retained from the original mask alignment system. Rotating the mask holder itself corrects for angular alignment errors, see Figure 21. A polycarbonate substrate, **(E)**, is glued onto a moveable bottom portion comprising a flat stainless steel structure **(C)** and a removable aluminum plate **(D)** secured with four screws. An O-ring provides a seal between the moveable bottom portion (**C** and **D**) and the chamber walls **(A)** to prevent leakage of liquid monomer into the inner mechanism of the fabrication chamber. The reaction environment is completely enclosed with a photomask supported on a glass plate **(B)**. A sensor tracks the absolute position of the bottom section (not shown).

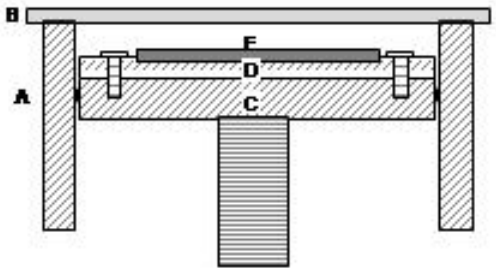

Figure 21 Schematic of the custom-built CLiPP-fabrication chamber, tooling set 2.

The second tooling set used for most devices presented in this thesis is shown in Figure 22. In Figure 22 **a)** the entire tool mounted on a slide is shown and in Figure 22 **b**) a detailed view of the in-house built fabrication chamber is shown.

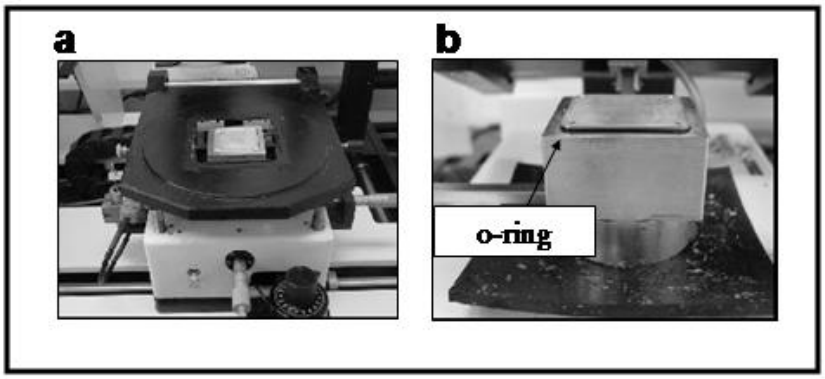

Figure 22 The second tooling set

The specific characteristics of the second tooling tooling set used with a modified OAI 200 mask alignment system are shown in Table 2.

Table 2 Characteristic features of the second tooling set, all units in μm.

Minimum feature resolution	Alignment accuracy*	Layer thickness accuracy†	Maximum‡/minimum thickness
20	**±10**	**±30**	**3000 /60**

* Determined by microscopy inspection
† Determined by profilometry
‡ Total device thickness

Evaluation of the second tooling set

Tapering of layers was still the major problem in the CLiPP process. This is due to the geometrical constraints imposed by a hinged mask that approaches a flat surface. When the mask is lowered, it touches the back side of the curing chamber first and, due to the rigidity of the glass plate, it is suspended above the front side of the curing chamber. Therefore, a cured layer is invariably thicker in the front than in the back. The tapering is not constant because of the varying thickness of the polymeric mask assembly, and has to be measured for each layer.

Another difficulty was that the angular control, θ, had to be removed to accommodate the relatively bulky tooling set. To correct for angular errors during the alignment, the whole mask needed to be turned. This made alignment cumbersome and difficult to reproduce.

The sliding mechanism, where the whole tooling set up is moved between the sample loading position and the exposure position, posed some problems. If moved too rapidly, the mask would occasionally get misaligned, which was only noted after the layer was polymerized.

5.4.3. Third Tooling Set

The principles established in the first and second tooling set was applied to a semiautomated mask alignment system, the 500J from OAI Inc. In this system, which is the current tooling set, better control over the tapering, retained angular alignment capabilities and swinging exposure system slide was wished for. Figure 23 shows a schematic of the current system where vacuum lines and general geometry are indicated and Figure 24 shows a picture of the set-up. Note the lack of retaining walls as opposed to the second tooling set.

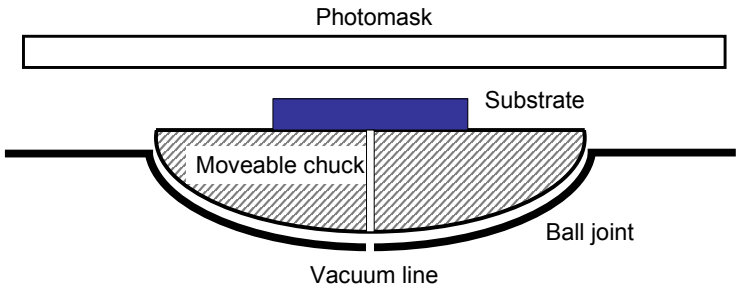

Figure 23 Schematic of the current tooling set up. The substrate is secured via vacuum, and the chuck is free to swivel on a ball bearing joint.

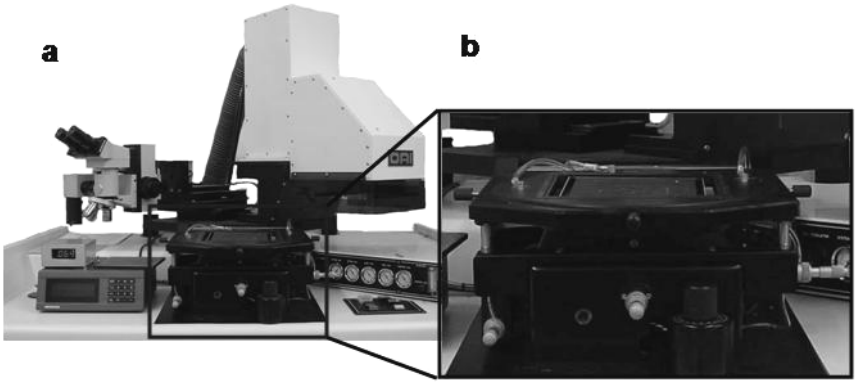

Figure 24 ***a)*** *The third and current tooling set.* ***b)*** *The magnified CLiPP-specific features that reside in the tooling section.*

In this system, the chuck, i.e. the base where the sample is held, is not in a fixed plane, but swivels on a ball joint. This joint is moveable when pressurized air is pushed through the system, and locked when vacuum is applied. Thus, tapering is controlled by contacting the mask with the substrate while the ball joint is disengaged. When level with the mask, vacuum is applied and the chuck is locked into position, see Figure 25. The substrate is contacted with the mask and the ball joint is in; **a)** open position, **b)** locked position.

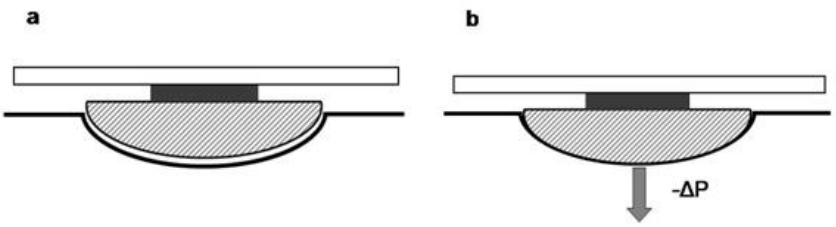

Figure 25 The ball joint in the current tooling set up.

The desire for a static curing chamber was solved by basing the system on the OAI 500J model. This model allows for movement of the light source and the microscope, while the curing chamber is in a locked position. Thus, when the sample is loaded, the light source swings into position, while the sample is fixed.

Due to the increased space available, the angular control is retained, which ensures facile alignment of layers. The specific characteristics of the third tooling set based on the OAI 500 J mask alignment system are shown in Table 3.

Table 3 Characteristic features of the third tooling set, all units in μm.

Minimum feature resolution	Alignment accuracy*	Layer thickness accuracy†	Maximum‡/minimum thickness
20	**±10**	**±10**	**5000μm/20**

* Determined by microscopy inspection
† Determined by profilometry
‡ Total device thickness

Evaluation of the third tooling set

The performance of the third tooling set is satisfactory in most respects. The main remaining problem is the thickness of the first layer, which is invariably thinner than desired. The main issue seems to be the pressure between the mask and substrate needed for contact detection, which lifts the mask slightly. When the chuck is lowered, the mask recovers its position, resulting in a reduced gap between the substrate and the mask. A more sensitive method for determination of the point of contact between the substrate and mask will be a marked improvement.

5.5. CLiPP Fabrication

Most devices presented in this work were made with the second tooling set, and fabrication specifics for this tooling set can be found in Papers I, II and V. This section relates to the third and current tooling set. The reasons for presenting the current system

are twofold. First, it has not been described in the literature yet since it came on line in late 2004. Secondly, it is commercially available and readily used by other research groups.

5.5.1. The CLiPP Process

CLiPP is a photolithographic process that uses masks and a collimated light source to selectively polymerize μm-sized features of predetermined thicknesses. Masks are printed on transparency films with a high-resolution commercial printer. Resolution is ca. 20 μm with this method, which is typically sufficient for microfluidic applications that have characteristic length scales on the order of 100 μm.

The following sections detail the methods with which one layer is produced and how 3D geometries are fabricated through sequential polymerization of single layers.

5.5.2. Fabrication Scheme of Single Layer Devices

A typical process for constructing a single layer starts with a substrate (usually a thermoplastic sheet cut to size, e.g. PMMA or Polycarbonate) secured in place via vacuum on the moveable bottom plate and a photomask attached with a viscous transparent liquid, e.g. PEG 400 or mineral oil, on a glass plate.

The substrate is raised until the top of the substrate contacts with the mask. The ball joint is in the open position, which ensures that the substrate levels with the mask plane. The ball joint is locked with vacuum, which ensures planarity throughout the rest of the process. While in contact with the mask, the lateral position of the substrate is measured with an absolute height sensor, giving an accurate positional reading of the substrate's upper surface. The substrate is now lowered until there is a large gap formed between the top of the substrate and the mask plane. The mask is attached on a hinged mask holder so it can be temporarily lifted from the curing chamber. When the mask holder, with the mask firmly secured, is raised out of the way, liquid polymer precursor is poured onto the substrate and subsequently the mask is lowered in place. The chuck is raised carefully until the monomer contacts the mask and spreads over the entire substrate surface in the course of raising the substrate to the desired position. The monomer is now confined between the mask plane and the substrate plane, defining the surface features and thickness of the layer. The polymeric precursor is a negative type photoresist where masked regions remain in the liquid state. When exposed with collimated UV-light, monomer in sections where the mask is transparent polymerize, forming an insoluble polymer network. The mask is removed and excess material, i.e. non-cured polymer precursor, is rinsed out with methanol and pressurized air, resulting in a layer of predetermined thickness having features corresponding to the negative image of the photomask, see Figure 26.

In Figure 26 **(a),** a chuck assembly with vacuum lines is shown. **(b)** Thermoplastic substrate attached via vacuum. **(c)** the chuck assembly is lifted until the top of the substrate touches the photomask and a zero layer thickness is set. **(d)** the mask is lifted and monomer is poured onto the substrate. **(e)** the chuck is lifted until the desired thickness is reached and the monomer is flood exposed with UV-light. **(f)** cured feature immersed in liquid monomer. **(g)** solvent rinsing of the structure. **(h)** finished structure. Sample single layer structures are shown in Figure 27. A single layer 65 μm trench with a height of 200 μms (aspect ratio of 3) fabricated with the first tooling set, **a)** A. The striations in the picture are due to the 15 μm pixels that the mask features are constructed from (5080 dpi printer). In **b)** 240 μm thick liver cell scaffolds with an array of 300 μm holes is shown, with one of the holes shown in detail **c)**. The liver cell scaffold is fabricated with the second tooling set.

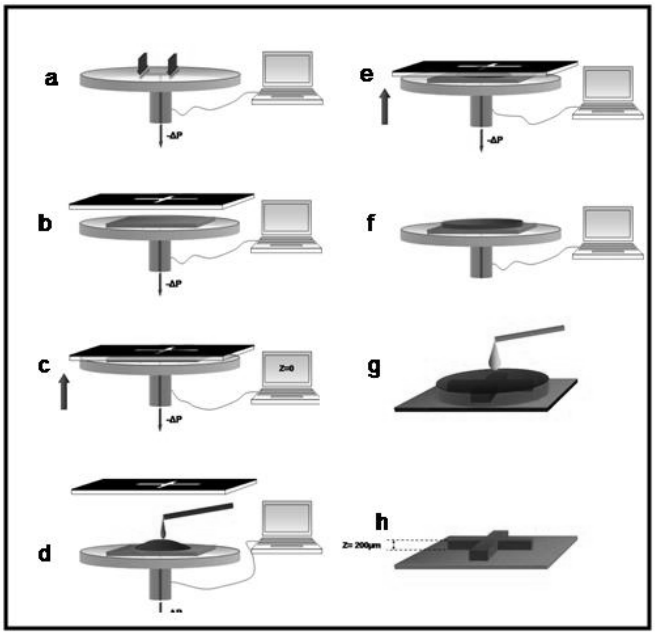

Figure 26 Fabrication sequence for a single layer.

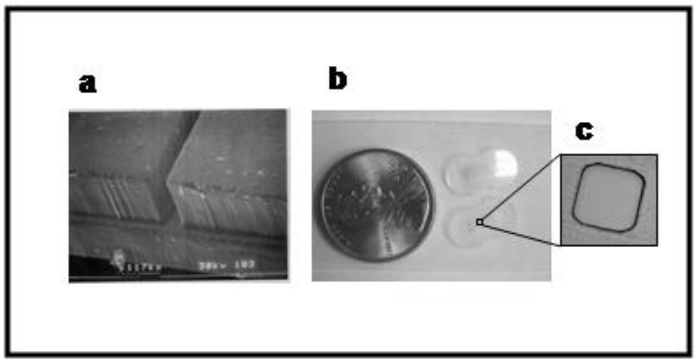

Figure 27 Examples of one layer devices. (The Author)

5.5.3. Multilayer Structures

Microfluidic applications generally require extensive channel systems. Channels are 3D objects, and depending on the fabrication method, two to three polymerized layers are needed for their construction. Multilayer devices present unique fabrication challenges. State-of-the-art processes typically employ fabrication of individual layers out of thermoplastic polymers, glass, silicon or PDMS and subsequent alignment and bonding of the layers in order to form functional 3D geometries, see Section 3.2.

However, the CLiPP scheme allows for covalent bonding between adjacent layers as the liquid polymer precursor is cured, rendering a separate bonding step superfluous. The use of a curable liquid formulation directly in contact with a layer that has trenches and voids poses significant challenges as blocking of previously formed features is not permitted. One possible way of solving this problem is to mask the liquid so that it is prevented from curing in the void sections, and while this works in some cases, it is impossible to form enclosed channels or other undercut geometries in this manner. A transfer scheme has been devised to address these challenges while retaining the basic idea of CLiPP, which is the formation of monolithic, seamlessly integrated multilayer devices without separate alignment and bonding steps.

Fabrication via the transfer method

The fabrication of the enclosed channel layer is performed by the transfer from the photomask of a previously polymerized top section. This method relies on polymerizing separately the top and the bottom layers of a 3 layer device, which are assembled in a sandwich configuration. When exposed, the middle layer is polymerized and covalently bonded to the top and the bottom layers. After removing the uncured monomer that resides in the device features with pressurized air and methanol, the device is finished. . In this manner, the whole sandwich assembly constitutes a covalently bonded monolithic structure.

In Figure 28 **(a)** Monomer is poured onto a photomask. The substrate photomask is later used to define the middle layer. **(b)** UV-exposure of the top layer in the three layer assembly. **(c)** Finished top layer attached to the mask that defines the middle layer. **(d)** A previously polymerized bottom layer is placed in the chuck assembly, monomer is poured onto it and the mask with the attached top layer finishes the sandwich construct. **(e)** Finished 3 layer device.

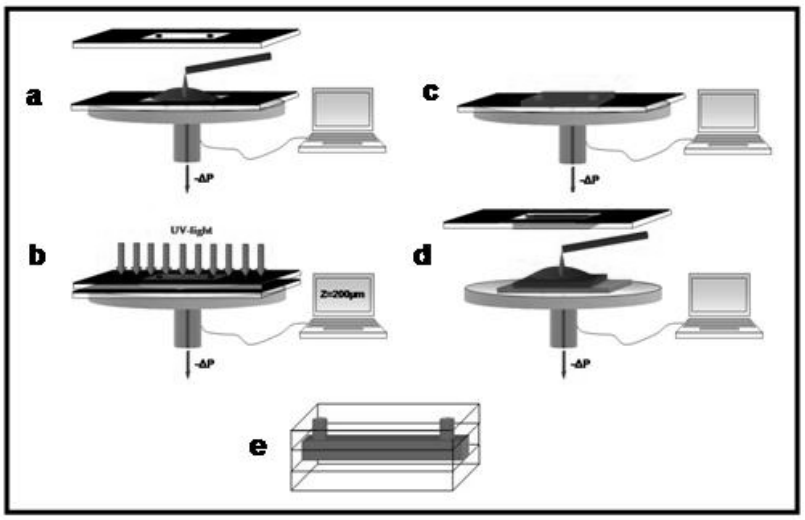

Figure 28 Fabrication of a channel layer via the transfer method.

In Figure 29 a device fabricated via the transfer method is shown. Note the nipples for facile connections to external equipment via tubing. The fabrication of such structures is discussed in 6.3.

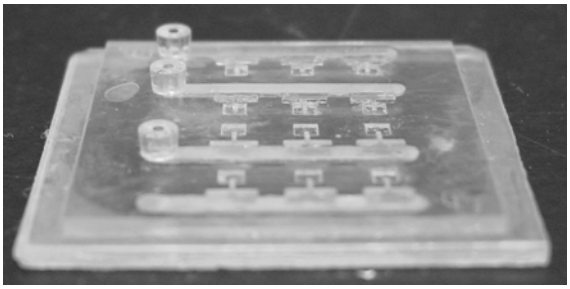

Figure 29 Device fabricated via the transfer technique. (Brian Good.)

Fabrication via sacrificial materials

To date, only the second tooling set has been utilized for 3 D devices fabricated via the sacrificial layer technique. Therefore schematics and text refer to this tooling set. However, the steps described are almost identical to what they would be in the third tooling set.

The basic idea in this technique is to exclude certain volumes in the device with sacrificial material, deposit structures around them and subsequently free the desired structures by preferential removal of the sacrificial layer. In this manner, channels and other void volumes are easily obtained. In the CLiPP process this scheme is currently realized through the use of a histology wax (Paramat Extra, Electron Microscopy Sciences, Fort Washington, PA) as the sacrificial material. A schematic representation of the processing steps is shown in Figure 30. Figure 30 **(a),** the aluminum plate, with the substrate and the first polymerized layer, is detached from the fabrication chamber and placed on a hot plate. Melted wax is poured on top of the heated assembly and quickly fills voids and cavities. The surface is leveled with a razor blade, leaving only a thin wax layer on top of the structure while cavities are completely filled. **(b),** a solvent polish step removes the thin wax layer, ensuring good adhesion to the subsequent layer. **(c),** the aluminum plate is repositioned in the fabrication chamber and steps shown in Figure 26 are performed to build the top layer. **(d)**, the final structure is released when the detached substrate is subjected to hot solvent and pressure, removing the wax, leaving a monolithic polymeric structure. For temperatures and other processing details, see Paper II.

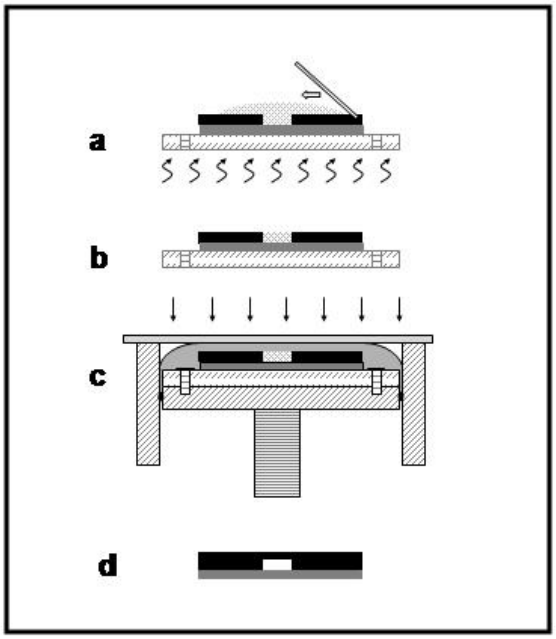

Figure 30 Schematic of the procedure for the fabrication of multi layer devices.

In Figure 31, two devices fabricated via the sacrificial layer technique are shown. **a)** An SEM picture of 500 μm thick structure composed of 400 μm wide bars on top of bars, fabricated with the first tooling set. This geometry would require multiple assembly steps if fabricated from premade structures. **b)** An optical microscopy picture showing 700 μm long buffaloes on a pedestal structure. 400 of these undercut microstructures were fabricated simultaneously using the second tooling set.

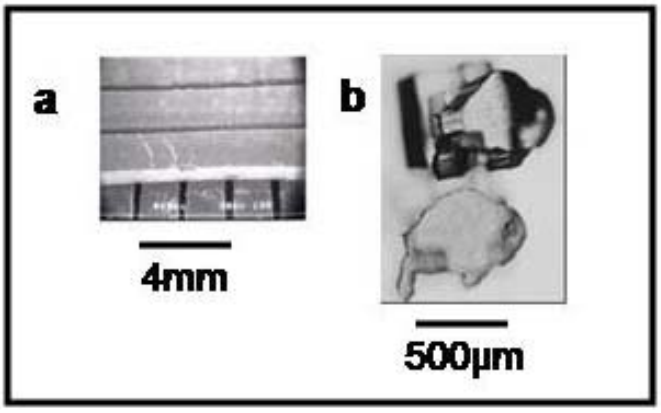

Figure 31 Structures obtained using the sacrificial wax technique. (The Author)

In the next chapter, the hardware and fabrication techniques for the fabrication of 3D structures, improved bulk materials selection and surface modifications are shown with several examples followed by discussions on these topics.

6. CLiPP Features

In this chapter, many features that are solved with the CLiPP technology are presented:

- Geometrical capabilities (papers I, II and V)
  - *3D capabilities*
  - *Independently moveable parts*
  - *Facile access to external equipment*
- Device material properties (papers I and V)
  - *Many different mechanical properties available*
  - *Hydrophilic/hydrophobic materials*
- Fabrication (Paper I)
  - *Incorporation of prefabricated structures and non-polymeric materials*
  - *Batch capabilities*
- Surface modifications (paper I and unpublished results)
  - *Biological compatibility*

6.1. 3D Capabilities

3D capabilities refer to complex devices where arbitrary points in a device are accessed from arbitrarily selected device locations. Such features are important for multiplexed designs where fluid ducts need to pass each other without crossing, i.e. without the fluids getting in physical contact. One such potential application is multiplexed flow cytometry,[59] where cells of interest are diverted by a laser beam into an accumulation area and cells of different types are diverted to a common waste receptacle. For device miniaturization, these streams must pass each other without any risk of crosscontamination.

In Figure 32 **a)** a maze constructed from 5 sequentially polymerized layers is shown. The mazes are each in a separate layer, and the maze seen at the top of the picture is actually two (optically) superimposed mazes, where one is located in the bottom structural layer and in the other resides in the top structural layer. A middle, transparent layer acts as a separation barrier. This device was made with the first tooling set.

In Figure 32 **b)**, further explained in paper II, a device with three intertwined channels is presented. Note in **b)** that the color sequence changes from the one order in the periphery to the order in the middle of the device. This is achieved by channel crossing with separate channel structures for each colored flow. This device was made with the second tooling set.

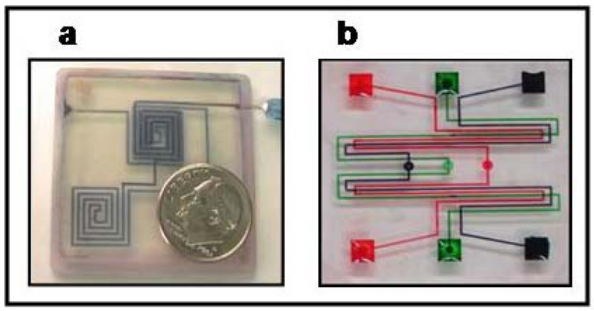

Figure 32 3D maze structures (the Author)

6.2. Independently Moveable Parts

In some instances, moveable parts are essential, although not favored by the scaling laws, see Section 2.1.1. Many microfluidic designs require dynamic valving and on chip pumping. Sometimes these unit operations are constructed with moveable flaps[60] and plugs[61].

To investigate the CLiPP capabilities for moveable parts, a cogwheel set up was designed and fabricated, see Figure 33. In **a)** dark colored wax is seen before solvent rinsing and release of the cogwheel. In **b)** and **c)**, the moveability is shown by the deformation of an air bubble residing in the colored stream.

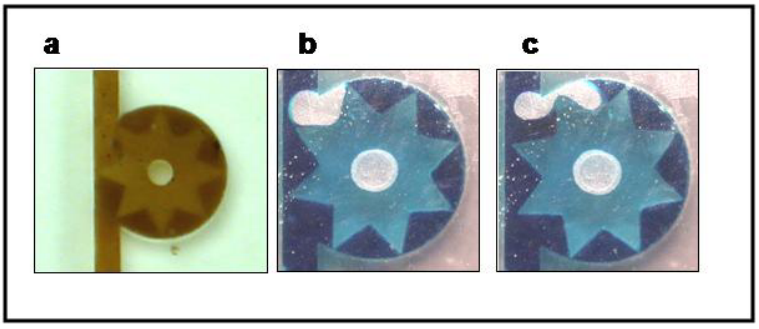

Figure 33 A moveable cogwheel (the Author)

It should be noted that the current precision in the CLiPP method is not sufficient to fabricate parts that move without substantial friction. This is partially due to the mask resolution, which, in the example showed in Figure 33, provides many interlocking and jagged features between the wheel and the post in the cogwheel device. The relatively low

precision is also partially due too the rough surfaces that the sacrificial wax layers provide. Therefore, a gap between the wheel and the top and bottom is quite large to ensure that the cogwheel is not stuck. This gap is seen in **a)** and **b)**, where a thin layer of fluid colors the top and the bottom of the cogwheel.

6.3. Large Structures for Facile Access to External Equipment

A critical factor for the function of microfluidic devices is the manner in which connections to microscopic equipment is performed. Since CLiPP allows for photolithography of very thick layers (currently in excess of 2 mm), it was realized that nipple structures for connections to tubing could be fabricated, see Figure 34.

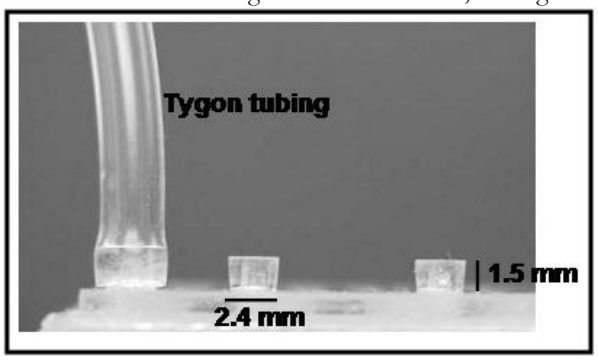

Figure 34. Nipple structures for reversible attachment of tubing fabricated via CLiPP. (the Author and Brian Good)

A few characteristics of these attachment structures are worth noting. First, the structures are very tall, 1.5 mm, which leads to significant light attenuation during fabrication as the UV-light passes through the polymerizing layer. The result is tapering due to the oxygen inhibition, see Section 7.3.1. This tapering is beneficial if the top portion of the structure is made slightly larger than the tube's inner diameter. In this case, the tube stretches over the top and follows the tapering all the way down to the device interface, which ensures leak free interfacing.

Secondly, the geometrical freedom of CLiPP allow for interface structures of different sizes to be fabricated simultaneously. In this manner, different sized nipples are independently positioned on the surface of the device, as required by the connections to external equipment.

Thirdly, the living radical process ensures good covalent bonding, see Section 6.9 between the interface structures and the device plane.

6.4. CLiPP Bulk Materials

It was shown in Chapter 3 that particularly two techniques have gained popularity for fabrication of complex polymeric devices in the microfluidics community; i) soft lithography; and ii). microfluidic tectonics. Briefly, it was shown that soft lithography techniques typically utilize silicon rubber (PDMS), which is very limited as a sole device material due to low mechanical integrity, poor resistance to diffusion and lack of robust

surface modification techniques, while microfluidic tectonics enables many construction materials but is best suited for three-layer devices, i.e. devices constructed from a top and a bottom layer with a channel layer between.

The CLiPP technology allows for the use of a nearly unlimited number of monomer compositions since the patterning and thickness control is unaffected by surface interactions and viscosity. Thus, highly viscous (similar to heavy cooking oil) formulations are polymerized in the same thickness range as are low viscosity (similar to water) formulations. Thus, the choice of monomer composition is almost exclusively controlled by the desired end properties.

Furthermore, different monomer functionalities are exploited in CLiPP for reduced residual stresses, improved patterning, tailored moduli and environmental friendliness.

A summary of the different functionalities utilized, to date, in CLiPP and their inherent advantages and drawbacks are presented in, Appendix A.

6.5. Multiple Materials

The CLiPP process enables control of the chemical and mechanical properties of each layer or section within a single device (e.g. channels, valves and separation media.) via the numerous vinyl-containing monomers available. Monomer selection impacts polymer properties such as optical clarity, modulus, toughness, swelling properties, and specific reactions with analytes or reagents. In Figure 35, a complex 3 dimensional brain slice perfusion chamber fabricated from two different materials is shown. **a)** The bulk of the device was fabricated from the standard, hydrophilic, acrylate formulation. **b)** Shows a close examination of each outlet port fabricated from a hydrophobic fluorinated monomer mixture, which was used for improved release from the mask.

Details on the fabrication and utility of this particular example are presented in Chapter 8.

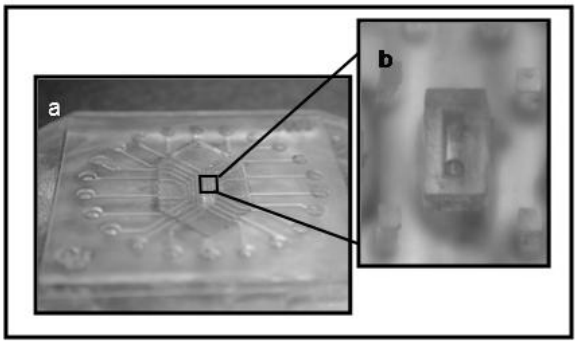

Figure 35 CLiPP-fabricated brain slice perfusiondevice with two different bulk materials.(the Author)

6.6. Incorporation of Prefabricated Structures

While photopolymerization is a very versatile technology with many possibilities to tailor the materials end properties, certain features necessary for successful devices are difficult

to achieve. The CLiPP technology not only allows for different materials in a single device, also prefabricated materials are easily incorporated.

Often in analytical field applications, complex sample matrices need to be processed, e.g. concentrated and purified, before proper analysis of target molecules is performed. For this purpose, filters with carefully selected functions are used. The ability to seamlessly incorporate filters in polymeric devices is a significant advantage in CLiPP since no clamping pressure, leakage prone O-rings etc. need to be employed to ensure that the liquid sample passes through the filter, and not around it, see Figure 36 and Figure 37. Figure 36 **a)**, using the CLiPP method, the filter, symbolized by the mesh pattern, is surrounded by the matrix, and access ports are created via photolithography, upper structure is a side view and the bottom is a top view. **b)** With alternative assembly methods, O-rings and a substantial clamping pressure is used to ensure a leakage free filter fitting. This device is made up of four discrete components, two structural layers and a filter with an O-ring sandwiched between them. In Figure 37, hepatocyte growth chambers, designed by Linda Griffith and Karel Domansky at MIT,[62] are polymerized on top of a filter selected for its mesh size and surface properties. This structure corresponds to the schematic shown in Figure 36 **a)**.

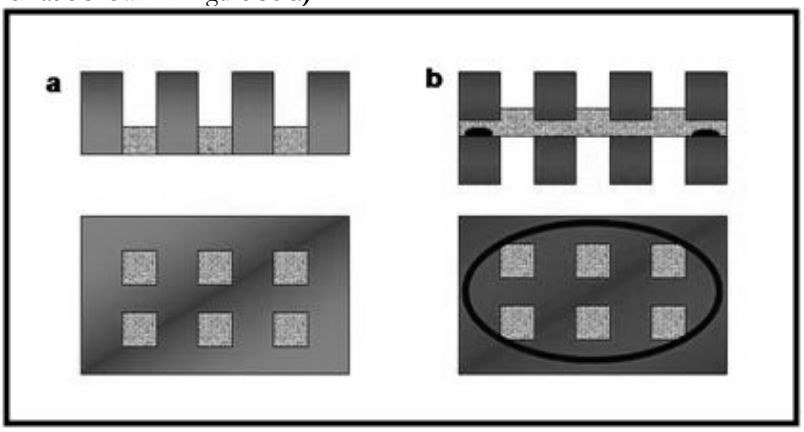

Figure 36 Schematic of filter incorporation.

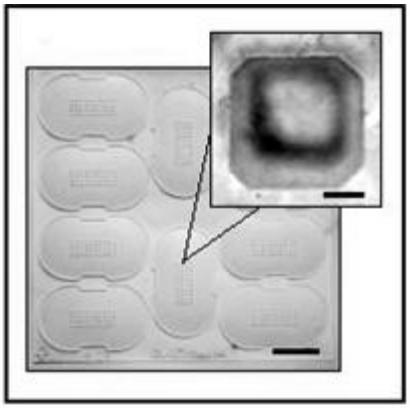

Figure 37 A cell culture chip designed by MIT with a filter incorporated, fabricated with the second tooling set. (the Author)

The cell culture chip in Figure 37 shows a CLiPP solution that minimizes the number of layers necessary for filter functions. In addition to streamlined fabrication, the properties of the single layer device are marked improvements over the assembled solution. First, there is no crosscontamination between the hepatocyte chambers since they are separated by a polymer material that is impermeable even over long time scales. This may be very important in future multiplexed solutions, i.e. many experiments run in parallel with separated perfusion systems. Secondly, the lack of assembly steps ensures facile, and thus less error prone, fabrication. Thirdly, the filter is fixed in position once the chambers are fabricated. Therefore no sliding of the filter is possible, ensuring robustness and integrity even when the filter device is subjected to high shear forces during seeding of cells and pumping of perfusate.

6.7. Batch Processing Capabilities

The filter hybrid device represents not only an important example of CLiPP versatility, but also shows the batch processing of CLiPP. In this case, the filter device was fabricated in batches of 10. Conceptually, the fabrication area is easily increased and the time consumption per device is inversely proportional to the fabrication area. Thus, low cost devices are expected to be produced in future fabrication tooling set-ups that fully utilize automation and large fabrication areas.

The batch capability was taken to its extreme by fabricating 400 undercut three layer structures; buffaloes on pedestals, see Figure 38. **a)** The main picture shows the structures prior to release from the sacrificial wax encasement. **b)** A single buffalo is shown in the bottom image. The right images show the intersections of: **c)** four pedestal bases, **d)** the cross-shaped pedestals, and **(e)** the same level after filling with molten wax prior to photolithographic polymerization of the CU Buffalo logo. The completed 400-buffalo matrix yields ca. 99% unblemished pieces. Scale bars: **a,** 3 mm; **b-e**, 300 μm.

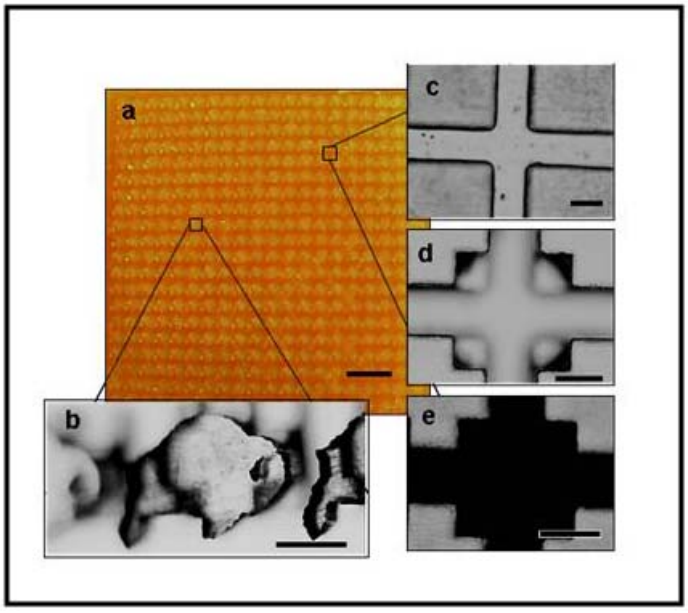

Figure 38 "Buffalo Herd." 400 microscale, three-dimensional Colorado Buffalo logos on pedestals are constructed in three layers to demonstrate applicability of the CLiPP process to massively parallel fabrication. (the Author)

The fabrication of the buffaloes used the sacrificial wax layer techniques, but could also have been made via the transfer method. The wax method was preferred because of alignment difficulties of the thick buffalo layer to the pedestal base layer. In future fabrication set-ups other means of indexation and alignment may alleviate these difficulties.

6.8. Backfilling of Trenches

The ability to integrate specialized materials into polymeric devices enables functionality that is not possible by using only polymer materials. The ability to incorporate non-polymeric materials into devices for microfluidic applications has been demonstrated using the CLiPP method in combination with trench backfilling, see Paper I. In Figure 39 **a),** conductive silver is polymerized into a multi-layer device and connected to a 3V watch battery and a LED bulb. Filling the fluid reservoir with an electrolyte solution illuminates the bulb. In **b),** a polymerizable carbon filament is incorporated within a two-layer device is shown. The thermotropic liquid crystal film indicates spatially-resolved heating of the device. Temperatures up to 90 °C were obtained by applying 115 V to the circuit. These conductive materials were filled into trenches that were fabricated in the base layer of the device. By using commercially available products, minimal development is required to construct highly value added products for microfluidic applications.

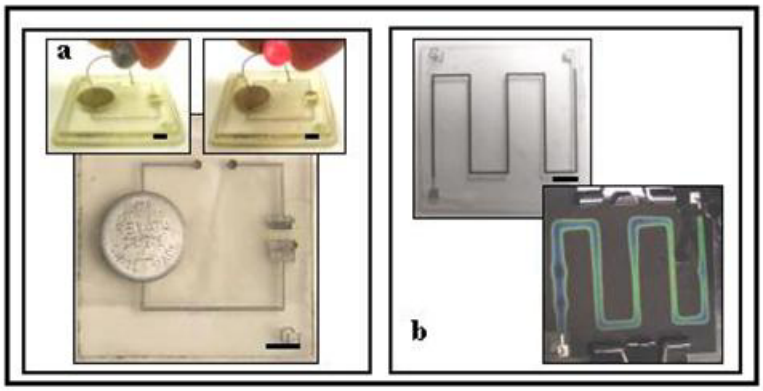

Figure 39 Pictures of devices utilizing existing materials. Scale bars: ***a)and b)*** *5 mm (Brian Good)*

6.9. CLiPP Surface Modifications and Interlayer Bonding

Many living radical modification schemes have been utilized for surface modifications of polymers. Among the more interesting surface modification schemes for patterned polymers is a work presented by Germack *et al.*[63] Here, subμm structures have living radical initiators distributed over the surface, enabling surface modifications similar to the CLiPP scheme.

The CLiPP process also depends on living radical photopolymerization (LRPP) processes for many of its advantageous features.[64,65] A schematic reaction sequence is shown in Figure 40. Here, two separate light mediated initiation events occur: cleavage of a photoinitiator and cleavage of TED (the iniferter used in CLiPP), forming a dithio carbamoyl radical (DTC). The photoinitiator radical fragment attacks a double bond, thus initiating polymerization. This monomer radical can either add other monomers or reversibly terminate with a DTC radical. The DTC capped monomer cleaves upon subsequent light absorption, reforming an active carbon based radical and a DTC radical. Relative to ordinary polymerizations monomers are added slowly due to rapid DTC-capping of radicals. Upon completion of the polymerization process, long polymer chains, or networks, capped with DTC groups are distributed throughout the polymer.

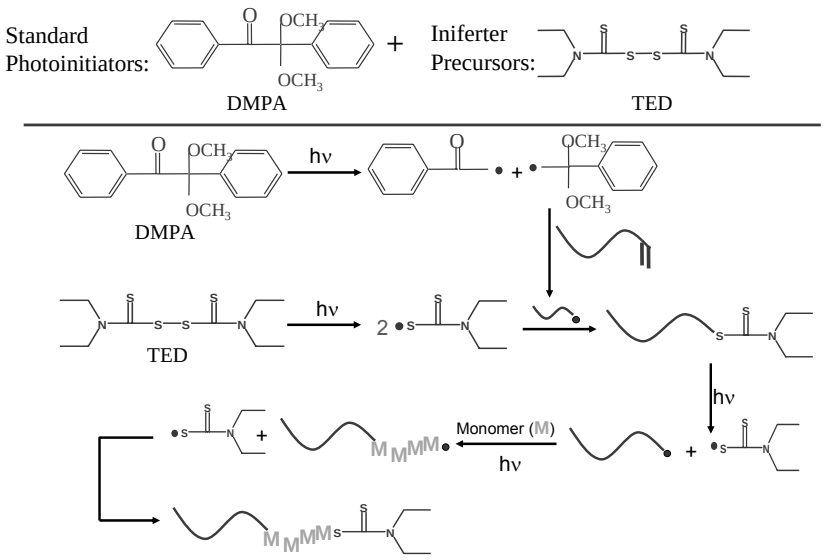

Figure 40 Living Radical PhotoPolymerization (LRPP) via TED (Figure Robert Sebra)

Incorporation of an iniferter in the monomer formulations enables covalent bonding between layers and spatially resolved grafting or modification via photolithographic methods, as seen in Figure 41. The structure to the left depicts a previously polymerized layer with reinitiable groups (DTC) attached to surface. When exposed to UV-light, these groups cleave, leaving active radicals tethered to the polymer matrix. These radicals initiate reactions with monomers in the immediate vicinity, i.e. the polymer precursor forming the next layer of the device, ensuring good covalent bonding between the layers.

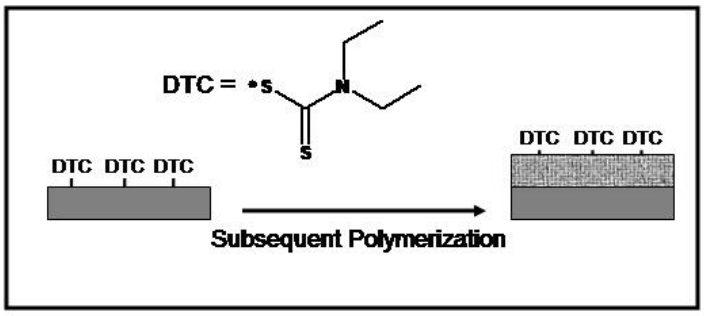

Figure 41 The living radical process as an adhesion promoter.

The LRPP process is general to many radically polymerized monomers and it is possible to first fabricate a polymer layer that consists of one monomer type, e.g. acrylates, and subsequently covalently bond a layer of another monomer type, e.g. thiol-enes. If so desired, portions of layers are constructed from one material and other portions of a

second material. The LRPP process ensures covalent bonding to all structural interfaces, i.e. sides as well as to the underlying layer.

Many functions performed in microfluidic devices rely upon interactions between fluids and transported chemical or biological compounds with the inner surfaces of the device. Often, spatially controlled surface properties that differ from the bulk material properties are desirable. A variety of monomers has been incorporated using TED to impart different surface characteristics. For example, Figure 42 demonstrates hydrophobic groups spatially grafted on the surface of a device. In Figure 42, dotted lines indicate fluorinated monomer grafted channels. When dyed water is flowed through the bottom channel, hydrophobic interactions with the lower right channel ensure a crossover to the upper channel.

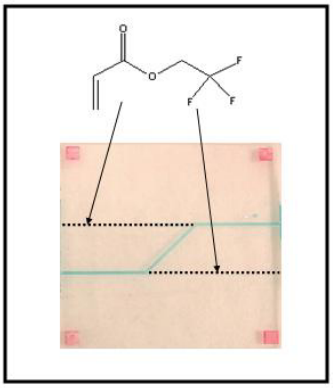

Figure 42 Hydrophobic modifications of channels (Robert Sebra)

6.9.1. Biological Compatibility

In many microfluidic applications, live tissue or individual cells are used. Inert environments are important in most biological research and non-toxicity to cells is a minimum requirement of microfluidic materials. In addition to non-toxicity, patterning of cells is of interest to separate different strains or different chemical environments without risking cross contamination due to cell growth or leakage of signal substances.

Cell compatibility and the effects of grafting are shown in Figure 43, where a PEG acrylate has been grafted via photolithography on the surface. It is clearly seen that cells prefer the unmodified surface to that of PEG. It should be noted that the layers are sufficiently thin to be undectable to the eye, and are only seen after staining the cells.

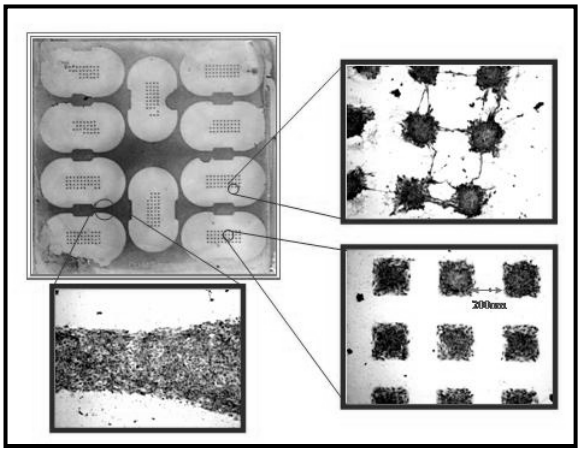

Figure 43 Patterning of Base substrate formulation grafted with PEG(375) monoacrylate patterns to prevent/guide cell attachment. (Robert Sebra)

The base matrix material is tolerated by cells for a significant time period. Cell scaffolds with hepatocyte 3D cultures that have grown for 2 weeks adhere to the device walls and show no sign of inhibited growth, see Figure 44. **a)** Shows the scaffold before seeding with cells. The small insert at the bottom right corner of the image shows CLiPP fabricated 20 μm holes used as an alternative to filters and **b)** shows a scaffold cavity seeded with a hepatocyte 3D culture after 2 weeks of growth in a specially designed perfusion chamber.

The morphology of the 3D cell culture was normal. It is therefore inferred that the unreacted monomer leakage from the device is below the toxicity threshold.

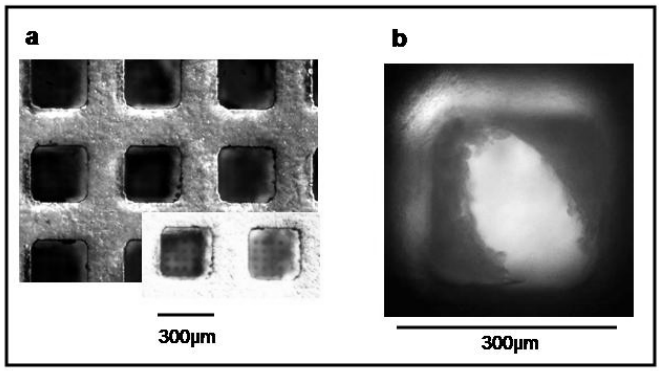

Figure 44 Cell scaffolds seeded with hepatocytes. Picture courtesy of Dr. Karel Domansky, MIT. (the author)

7. Patterning in CLiPP

In this chapter, photopolymerization phenomena that affect patterning quality in the CLiPP process are discussed. The role of inhibitors in 2-dimensional curing is qualitatively treated. Results from previous chapters are used to discuss patterning properties of different monomer types. In this chapter, definitions commonly used in descriptions of negative photoresist lithography are taken into account and applied to CLiPP monomers. The chapter concludes with observations on the benefits and drawbacks of specific monomer functionalities with respect to patterning in the CLiPP process.

7.1. Photoiniferter

As has been previously described, photoiniferters play a vital role in the CLiPP process: they ensure good adhesion between layers and other polymerized features: and provide a facile route for surface modifications of channel walls, detection pads etc. A few photoiniferters were evaluated during the course of the CLiPP development, but other iniferters than TED all had various drawbacks, ranging from poor reactivity to poor patterning properties.

The role of the iniferter is more complex than just adding living radical character to devices. Firstly, the presence of iniferters (TED) has been shown to change polymerization kinetics from α =0.5 to values close to 1,[66] which has implications on patterning properties. Secondly, iniferters are likely to affect patterning in a manner similar to oxygen.

7.2. Patterning

The phenomena that determine patterning, i.e. the quality of reproduction of mask features, are numerous and interact in very complex ways. Many of these factors are tooling dependent, while others are functions of polymerization kinetics and the actions of contaminants and additives. In the following sections, tooling dependent and independent factors are discussed.

7.2.1. Tooling Dependent Phenomena

The basis for the photochemical reaction is UV-light that is produced by a light bulb and focused on the substrate with optics. The optics determines the patterning quality of tall features, since poor optics introduces angular errors of the illuminating beam, i.e. poorly collimated light. Also, light that passes through the mask and into the monomer composition is refracted since the glass and monomer have different refractive indexes. Refraction also broadens the light beam.

The tooling dependent factors are relatively static, and are not expected to change significantly during the curing process. Non-step wise illumination is the basis for pattern

imperfections, since the presence of even low light intensities cause polymerization events outside of the desired area.

7.2.2. Tooling Independent Phenomena

Many dynamic processes are present during photolithographic polymerization. Mainly, these processes originate from kinetics and diffusion phenomena. The following sections detail these factors and gives qualitative explanations of their effect on pattern reproduction.

Inhibitors in a 2-dimensional system

The situation for 2 dimensional systems is much more complex than the uniformly exposed systems that were described in Chapter 4. First, the light intensity varies across the surface, due to the masking. Thus, portions of the monomer are fully exposed to light, whereas other portions remain unexposed. Secondly, optical effects, such as diffraction and refraction, lead to complex light geometries due to beam broadening phenomena. Therefore, finite amounts of light are present in masked portions of the polymerizing layer. Thirdly, unexposed regions behave as reservoirs for dissolved inhibitors, primarily oxygen, that freely diffuse into the polymerizing feature due to concentration differences imposed by inhibitor consumption in exposed areas, see Figure 45.

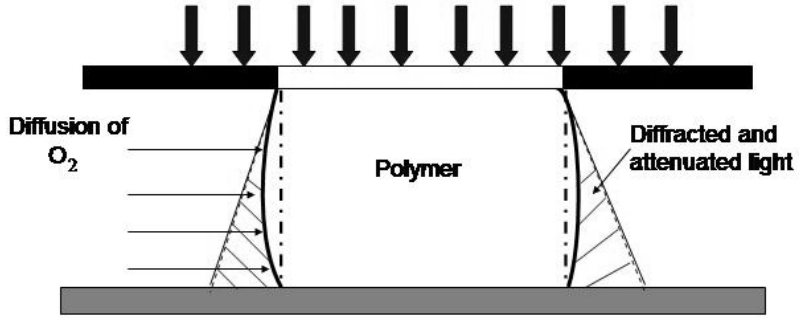

Figure 45 Dynamic phenomena in polymerization of a CLiPP structure.

A perfectly patterning monomer should exhibit the following polymerization properties:

- Fast polymerization at high light intensities
- Slow polymerization at low light intensities
- Initiator sensitive to inhibition reactions

7.3. Contrast

The primary role of the monomer formulation is to rapidly form an insoluble polymer with a predetermined shape. Different formulations solve this task more or less efficiently,

and to give this behavior a mathematical meaning for photoresists, contrast, γ_n, has been defined, see Eq. 7.1. [6]

$$\gamma_n = \left[\log \frac{D_g^0}{D_g^i} \right] \qquad \text{Eq. 7.1}$$

where γ_n is the contrast, D_g^0 is the dose required for polymerization of the desired shape throughout the feature thickness, i.e. vertical walls, and D_g^i is the dose required for gelation.

Thus, formulations with a rapid transition from a sol-state to a fully developed polymeric network exhibit good contrast, see Figure 46.

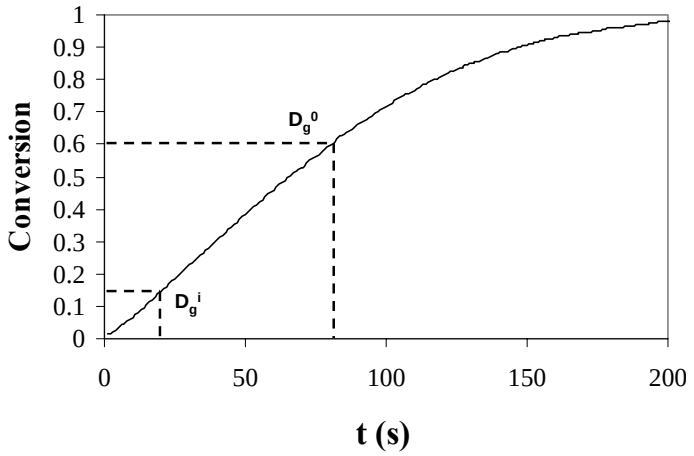

Figure 46 Relationship between the gelation dose and the dose required for acceptable mechanical properties.

In Figure 46, the gel point conversion and the conversion that corresponds to a network with fully developed mechanical properties are indicated. Note that the actual example shows a monovinyl system which does not develop any mechanical properties due to the lack of a network. The figure should therefore only be seen as an illustration of the contrast concept. Also note that the scale on the x-axis is in units of time and Dg^i and Dg^0 are in units of energy. These are related through $I_0t=D$, where I_0 is the light intensity, t is the time and D is the dose.

In a crosslinking system, gelation is reached at very low conversion. The exact gel point depends on the functionality of the monomers where a hexavinyl mixture gels at a lower conversion than a divinyl mixture. In multivinyl systems it is therefore the inhibition time before any polymerization occurs that controls the patterning fidelity.

7.3.1. The Role of Oxygen Inhibition

The oxygen inhibition process is one of the most important factors for patterning quality. The convex shape of the structure in Figure 45 is controlled by the relationship between radical production rate and oxygen inhibition. The light intensity has its lowest

value at the bottom of the film and the oxygen diffusion from adjacent monomer reservoirs is most effective.

Once the polymerization has reached the gel point, diffusion is decreased orders of magnitude and oxygen replenishment is effectively ended.[67] Therefore, when polymer structures have been formed, the remaining polymerizations inside the structures follow non-inibited kinetics and rapidly reach high conversions.

The important role of oxygen inhibition for good patterning can also lead to challenges. In a device where channels of 200 μm and 10 μm are fabricated at the same time, the oxygen will be depleted in the 10 μm channels first. Thus, the oxygen replenishment is still sufficient to delay unwanted gelation in the 200 μm channel, but insufficient in the 10 μm channel. In this case it is important that the monomer has a large difference in polymerization rate between high and low light intensities, i.e. a high α, to minimize feature broadening, see Section 4.2.2 and Appendix A.

7.3.2. The Role of TED

The role of the iniferter precursor TED is speculated to be twofold in CLiPP: Firstly, a diffusion driven effect that shares similar traits to oxygen inhibition: and secondly, an effect on the overall kinetics.

The TED reaction is initiated by UV light, similar to the photoinitiator initiation. The formed radicals reversible terminate carbon based radicals, see Section 6.9. In this manner, TED is consumed in polymerizing features. A concentration difference between the polymerizing features and adjacent monomer reservoirs is created and a flux of TED results. Therefore, there should be an increase of free and bound dithio carbamoyl, DTC, i.e. the group that results from TED cleavage, at the polymerizing feature's edge. Since all DTC groups remain active, rate of polymerization is lowered at the edge, which delays feature broadening. It should be noted that this explanation is tentative, and no measurements of DTC concentration at side walls have been conducted yet.

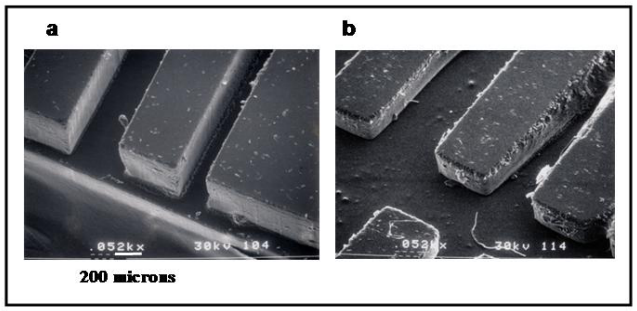

Figure 47 Comparison of features with and without TED

7.3.3. Monomers

Different monomer functionalities, e.g. methacrylates, acrylates and thiol-enes, have unique advantages and drawbacks in the CLiPP scheme. Below is found a brief summary of the tested formulation with respect to patterning. Again it should be pointed out that no scientific study of patterning properties has yet been conducted. The statements below should only be read as a compilation of CLiPP fabrication experience.

Acrylates

Acrylates have constituted the bulk of CLiPP applications. In combination with TED the patterning results are good.

Methacrylates

Initially, methacrylates were used as a matrix material, but were discontinued due to very poor patterning properties, even in the presence of TED.

Thiol-enes

Thiol-enes react very fast, an order of magnitude faster than acrylates, which makes it difficult to pattern from a process control point of view. Note that thiol-enes are not affected by oxygen inhibition thanks to very fast hydrogen abstraction reaction which leads to a chain wise consumption of oxygen molecules.

Vinyl ether maleates

Very good patterning results have been experienced with vinyl ether maleates with no abstractable hydrogens.

7.4. The Role of α for Patterning in CLiPP

It was shown earlier that oxygen inhibition and TED counters this effect through inhibition or iniferter mechanisms. In certain cases this effect abates due to oxygen and TED depletion in the liquid reservoirs adjacent to the polymerizing features. At that point polymerization kinetics gain in importance.

To minimize unwanted feature broadening, high α's are desirable. A simple example serves to illustrate this: if the light intensity is $1/100^{th}$ outside of the desired feature compared to at the feature, $\alpha = 1$ yields $1/100^{th}$ of the polymerization rate. Under the same conditions $\alpha = 0.5$ yields $1/10^{th}$ of the polymerization rate. This effect is shown graphically in Figure 48, where the black line is a plot of a photo-RTIR experiment on MHVE/DEMA and the gray line is a photo-RTIR plot of lauryl methacrylate (LMA). Two light intensities were used for each sample, 150 mW/cm^2 and 2.4 mW/cm^2. Indicated in the graph are conversion levels of 70% and 10%. See Paper IV for experimental details.

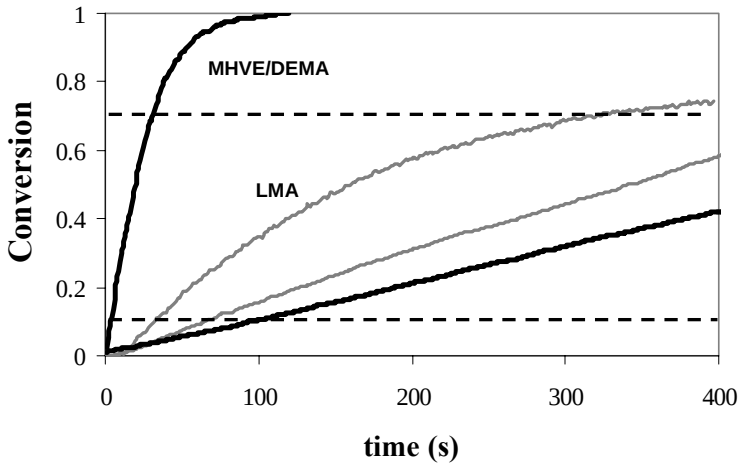

Figure 48 Conversion as a function of polymerization time for a vinyl ether maleate and a methacrylate at two light intensities.

In Figure 48 it is shown that the MHVE/DEMA mixture reaches 70% conversion at the high light intensity well in advance of reaching 10% at the low light intensity. The opposite is true for the methacrylate formulation, where 10% at the low light intensity is reached significantly earlier than 70% at the high light intensity. For patterning purposes, the vinyl ether maleate is expected to have superior performance.

7.4.1. The Effect of TED on Kinetics

Several studies have been conducted on the role of TED in various monomers. In thiol-enes, the effect of TED is an increase in α from 0.5 to 1.[68] Similar results were obtained with acrylates, where α increased from 0.5 to 1.[69] In methacrylates, TED had no effect on α. These differences in α between TED and non-TED containing monomer formulations are a likely explanation for the difference in patterning quality seen in Figure 47. Also, the lack of any kinetics effect of TED provides a rationale for the, so far, unsuccessful use of methacrylates in CLiPP.

8. A CLiPP Application

"The proof of the pudding is in the eating"

Often misquoted proverb from the 14th century

In this chapter, a brain slice perfusion device fabricated via CLiPP is presented. It represents an important example of the solutions that are possible with the new technology. This device is described in detail in Paper V.

8.1. Introduction

All new technologies have to be proven by meeting one or all of the following criteria; i) solving existing problems; ii) producing results less expensive than state of the art technologies; and iii) producing results faster than state of the art technologies. Unless the new technology has significant advantages in at least one of the above criteria, it will not be used.

To assess the utility of CLiPP, a novel brain slice perfusion device was fabricated. The specific advantages of CLiPP used in the fabrication are 3D capabilities and the facile incorporation of a second polymeric material. The brain slice perfusion device example also shows the speed with which new monomer formulations are evaluated. In the specific device, materials substitution was necessary to counter a problem where small structures broke off from the device during mask removal. This was solved in less than 6 hours via simple formulation changes.

8.2. Device Purpose

Neurological disorders are an increasing problem in the developing world as well as in the industrialized world, costing the society large amounts of resources for assistance, treatment, lost productivity and extracts a humanitarian toll through the suffering of affected people and their next of kin.

To elucidate the mechanisms for neurological ailments, brain slice devices that provide harvested brain tissue with nutrients to keep them viable, while simultaneously allowing for electrical or optical measurements of small regions of the slice have been designed. To date, rational research into the effects of therapeutic drugs or biological fluid in various limited regions of the affected brain has been difficult with current state of the art brain slice perfusion devices due to imprecise introduction, both spatially and volumetrically, of the studied drugs.

Progress has been made in research labs to alleviate imprecise nutrient and waste perfusion, and P.A. Passeraub *et al.* [70] has fabricated and characterized a perfusion chamber that ensures optimal nutrient supply in combination with a geometry that provides for facile electrical measurement of neurological activity.

An extension of this work, where the perfusion geometries are retained and a separate layer of fluidic connections allow for the pinpoint introduction of therapeutic drugs, is presented in this paper. This represents a significantly improved device for the elucidation of brain activity in response to drug exposure.

The necessary seamless integration of sequentially fabricated polymer layers and brain slice support posts are achieved through the use of a living radical process, which provides for covalent bonding between polymerized features.

This example details the use of CLiPP for the fabrication of a brain slice device with a complex 3D geometry. Specifically, the challenging task of providing geometries tailored to precise drug exposure to selected sites on a brain slice is discussed. Also, the channels are multiplexed with up to 8 different drugs administered locally and simultaneously, which provides for an efficient and flexible use of the perishable biological sample.

8.3. Device Design

The new device was designed to allow for pinpoint delivery of drugs while simultaneously allowing for facile electrical and optical measurements of one side of the brain tissue. Thus it is necessary to fabricate a device that has two separated flow systems, one for the perfusion flow and one for the drug delivery. Care must be taken to ensure that cross-contamination between these flow systems are minimized, i.e. the drug that is introduced into the device must be pumped to a waste container at the same rate as it is pumped to the brain slice. This necessitates a push-pull micropump solution. This is where one pump, in pushing mode, is connected via tubing to the drug introduction structure, and a second pump, in pulling mode, is connected to the waste, see Figure 49.

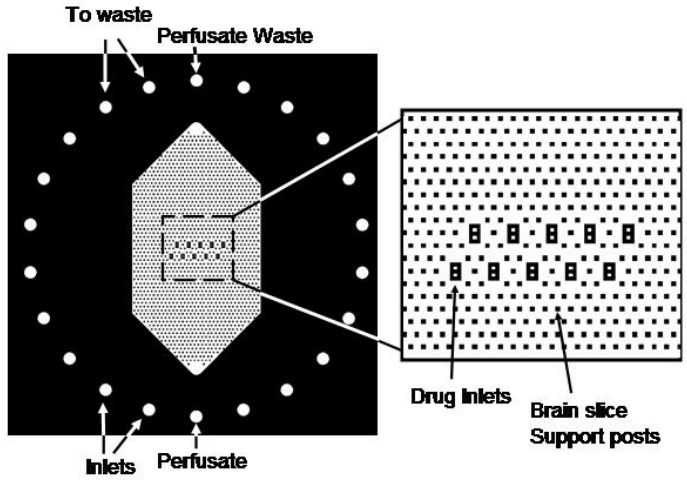

Figure 49 Design for the top layers of the multiplexed device. Dark portions are polymerized features and white portions show holes and the empty volume around the brain slice support posts.

The entrances at the very top and bottom in Figure 49 are for perfusate flow and the other entrances and exits are for microsyringes operating in a push/pull fashion. The fluid enters one drug inlet post, and exits through the same post. The fluidis then passed into a waste stream that ends in the opposing micropump, see Figure 50. Here, supporting posts are indicated in gray, and the semitransparent structure is the post containing two channels for drug introduction and disposal.

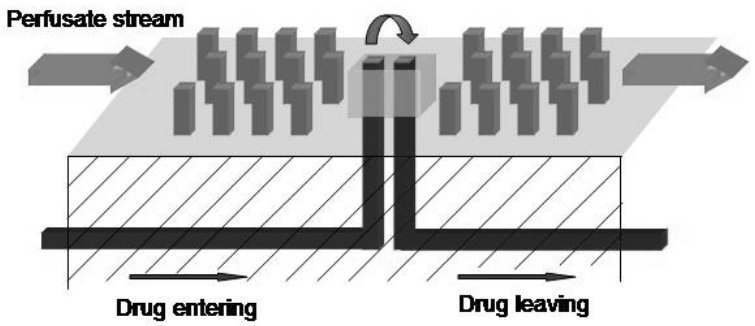

Figure 50 Schematic cross section of the drug delivery and waste system.

8.4. Experimental

The basic component of the experimental set up is a modified mask alignment system where a specially designed reaction chamber is incorporated to make polymerizations of thick, planar layers of liquid polymer precursors possible. For monomer formulations and detailed fabrication parameters, see Paper V.

8.4.1. Fabrication of the Brain Slice Device

The fabrication of the three lower layers were via the transfer method, see Section 5.5.3. Access points to the channels were plugged, and the two top layers were fabricated in a sequential fashion. Finally, the wax plugs were dissolved in warm methanol, releasing the finished device, see Figure 51 and Figure 52.

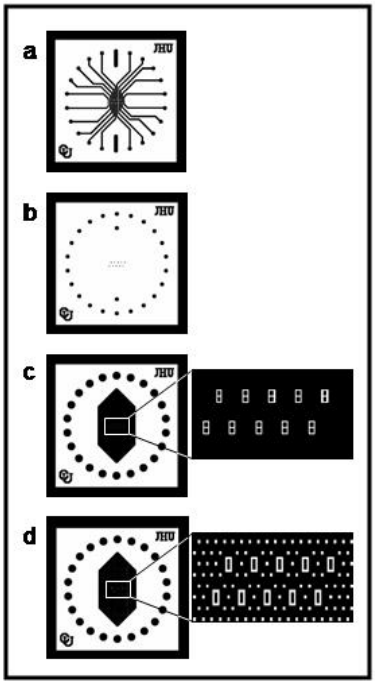

Figure 51 Mask sequence used for the brain slice device.

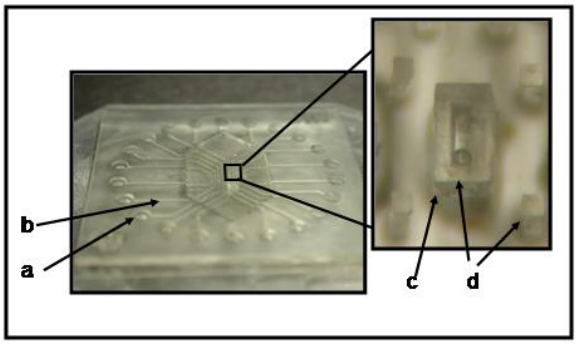

Figure 52 Finished device with individual layers, as denoted in Figure 51, indicated.

8.4.2. Polymerization Conditions

Polymerizations were conducted at ambient conditions using a medium density Hg-light source with a spectral output between 300 and 450 nm. No cut-off filters were used. The light intensity was set at 50 mW/cm^2. Typically, the curing time was 350 s, yielding a dose

of 17.5 J/cm^2. For the transfer step the curing time was increased to 500s, yielding a dose of 25 J/cm^2, to counter the added sample thickness.

8.5. Results and Discussion

8.5.1. Device Fabrication

The fabrication of posts caused significant difficulties due to adhesion to the acetate photomasks. Normally, 30-50% of the posts stuck to the mask instead of the device. A first approach to a solution of this problem was to strengthen the post material through higher crosslink densities, i.e. a larger amount of the hexafunctional oligomer. This did not appreciable lower the number of posts that failed. Subsequent tested solutions were; increased curing times, lowered amount of initiator to ensure an even cure through the posts and coating the photomask with release layers comprised of fluorinated alkanes or silianized alkanes. Ultimately, these efforts were not successful. The problem was finally solved by changing the monomeric composition of the liquid formulation. To ensure facile removal of the photomask, 50% (wt/wt) fluorinated acrylic oligomer was used together with 50% (wt/wt) reactive diluent (the exact formulation is found in section 2.1). With the aid of the fluorinated monomer 100% of the posts were released from the mask. The success of fluorinated formulations is likely attributed to the difference in surface energy of the acetate film, which is hydrophilic, and the hydrophobic polymer, which minimizes the adhesion forces.

8.5.2. Transfer Method

The transfer method has many advantages over previous sacrificial layer protocols, see Section 5.5.3. Previous, sacrificial layers had to be used to fill all the voids in the entire channel layer. Here, the transfer method provides for straight and planar geometries that are independent of the surface shape of the sacrificial layer. The channel thickness control is better than in alternative methods since sacrificial material shrinkage, and thus lowered channels, is avoided. Furthermore, the time consuming removal of sacrificial material in channels is avoided, and the structural integrity is ensured since no extensive melting and rinsing protocols to release the final device are necessary.

8.5.3. Covalent Adhesion

Covalent adhesion between layers is provided by living radical processes, see Section 6.9. Strong bonding is particularly important for the successful fabrication of the two-layer central posts, see Figure 52. The post's surface areas are small and the torques applied when the mask is peeled is significant. Therefore, in order to avoid delamination, the bonding forces need to be strong and the post interfaces to be free from unbonded portions.

8.5.4. Brain Slice Device and Auxiliary Set-up

The finished brain slice device contains many innovative features such as 1) facile connections to auxiliary equipment, 2) large unobstructed areas that allow access for a

variety of detection equipment, e.g. microelectron arrays and conventional glass-pulled microelectrode even in restricted area below microscopes, 3) unique perfusion structures for optimized nutrient and waste transport and 4) separated perfusion and drug fluid streams. These features are important since they minimize the need of harvesting of laboratory animals. In addition, the features ensure statistically relevant research results since the conditions are identical throughout the slice. Furthermore, the design facilitates connections to auxiliary equipment, see Figure 53.

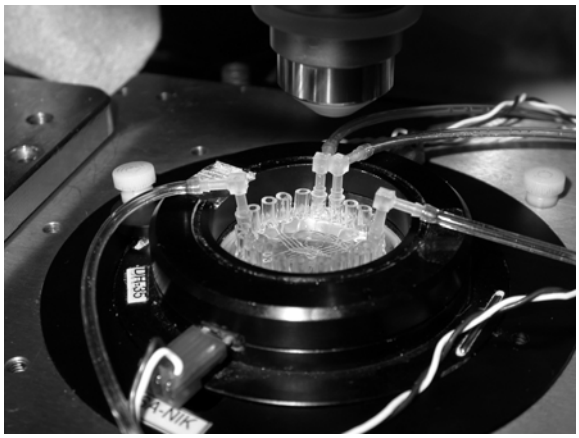

Figure 53 Two photon microscope set up with two micropumps attached.

8.5.5. Device Evaluation and Conclusions

The functionality of the brain slice device has been preliminarily evaluated by pumping of relevant biological fluids, such as nutrient solutions, through the drug access point posts, i.e. the large posts with two channels located in the middle of the brain slice chamber. These initial tests have revealed that the basic geometry is sound, but the materials need to be improved due to excess adsorption of biomolecules.

Future work will address the issue of surface properties to minimize adsorption. Subsequent generations of the brain slice device will be used in Epilepsy research on animal models. Future work will address the issue of surface properties to minimize adsorption of dissolved organic matter in the drug streams. The application of subsequent generations of the brain slice device may be found in the epilepsy research on animal models.

A final word about this 3D microfluidic device is that it illustrates the ability to access any portion from other parts of the device, resulting in optimal use of the allotted volume while reducing the cost of addressing demanding microfluidic operations.

9. Conclusions

9.1. General

Microfluidic devices have long been considered an ideal tool for rapid and inexpensive chemical analysis and molecular manipulation in areas ranging from point-of-care health applications to homeland security. To date, microfluidic solutions have been commercialized mainly for drug development end-users, where the main advantages are reduced reagent consumption and rapid reactions.

The microfluidics research community has developed many innovative solutions in a vast range of areas, but relatively few devices have entered the marketplace despite the efforts of many university spin offs and start ups over at least a decade. The main hurdles have been development expense and fabrication difficulties, especially in the area of complex, automated devices.

To date, the community has lacked a versatile process that minimizes the number of fabrication steps and the number of different microfabrication technologies that must be employed.

The main goal of the work presented here was to address this lack of fabrication versatility, and the goal has been met through the invention of Contact Liquid Photolithographic Polymerization (CLIPP).

9.2. Conclusions

9.2.1. CLiPP Solutions to Microfluidic Challenges

A number of microfluidic challenges that must be met by a general fabrication method have been identified:

Geometrical issues:

- *Facile microfluidic interconnections, i.e. chip-to-world interfaces*:
- *Efficient mixing of reactants in the predominantly laminar flows.*
- *Unwanted fluid flows due to large capillary forces.*
- *Prevention of fluid evaporation.*

Surface chemistry issues:

- *Prevention of unwanted adsorption of dissolved molecules.*
- *Prevention of clogging and blocking.*

It was shown that CLiPP is able to solve these problems via the following CLiPP abilities:

- Geometrical capabilities
  - *3D capabilities*
  - *Independently moveable parts*
  - *Facile access to external equipment*
- Device material properties
  - *Many different mechanical properties available*
  - *Hydrophilic/hydrophobic materials*
- Fabrication
  - *Incorporation of prefabricated structures and non-polymeric materials*
  - *Batch capabilities*
- Surface modifications
  - *Biological compatibility*

A specific real world application, a novel brain slice perfusion device, was presented to evaluate the potential of CLiPP. In this device, facile access to external equipment, 3D geometries and multiple materials were used to ensure simple interfacing and maximum research utility. This example illustrates important design concepts that are useful for a wide variety of devices.

9.2.2. The Role of Kinetics in CLiPP

In this thesis the kinetics for several monomer compositions has been presented. The kinetics for methacrylates and acrylates were found to follow literature values, which served as methods validations. Also, several vinyl ether/maleate copolymerizing compositions were studied. It was found that the presence of easily abstractable hydrogens lowers the dependence of polymerization rate on rate of initiation, i.e. a lowered coefficient α. The specific α's found follow literature values of other vinyl ether/maleate copolymerizations. In the absence of easily abstractable hydrogens, significantly higher α's were found. This is previously unreported in the literature. It is speculated that the major cause for the increase in α is chain length dependent propagation (CLDP).

Kinetic results were used to explain observed behaviors of different monomer types used in CLiPP. Using well accepted definitions for patterning properties it was shown that a high α is beneficial for good patterning.

It was also shown that inhibition reactions of oxygen and reversible inhibition of photoiniferter precursors are important for patterning properties.

10. Future Work

For CLiPP to become a major technique for rapid prototyping as well as mass scale fabrication, developments in many areas are necessary. Below, unique research devices where function is the greatest concern, and mass fabricated devices where cost is paramount, are discussed.

10.1. Unique (Research) Devices

The goal for CLiPP development for research applications is to strengthen and broaden the distinctive capabilities in fields that are recognized as difficult using state-of-the-art fabrication processes. Two important fields are materials development and integration of specialized components.

10.1.1. Materials Development

To date, the materials used in CLiPP are adaptations of commercially available lacquer formulations, thiol-enes and fluorinated monomers. Thus, only a very limited set of formulations have been tried and a vast number of possibilities remain. Development of specialized monomers for optical, electrical and biological applications is necessary for the integration of external equipment, e.g. lasers, and for the utility in biological research.

10.1.2. Integration of Sensors and Actuators

Many functions are best solved with IC-technology. To ensure compatibility with standard biological protocols and accepted analysis and detection methods, seamless incorporation of prefabricated sensors and actuators must be accomplished. Some early attempts to reversibly bind silicon microfluidic devices have been made via materials substitution. To date, permanent incorporation with tailored packaging of silicon devices have not been achieved in CLiPP.

10.2. Mass Production Capabilities

For CLiPP to become a successful alternative to current state-of-the-art fabrication technologies, major development of both methods and hard ware must be performed. The main weaknesses in the technology related to mass fabrication are:

- Liquid handling.
- Mask removal.
- Polymerization area.
- Cure time.

CLiPP is well suited for automation of the liquid handling. The polymerization area is also easily addressed. The cure time depends largely on the presence of the photoiniferter.

Development of monomer formulations that retain the benefits of the photoiniferter while shortening the cure time is a major challenge.

11. Acknowledgements

Many people and personalities constitute the main characters and supporting cast in the *film-noir* with a happy ending that was my PhD research.

Cast in order of appearance, Sweden:

Pär Ottoson Kalm: A man with a God-given talent for UV-lacquer formulations. He taught me the basics of UV-technology during a stint at Becker-Acroma, late last millennium.

Otto Öström, R&D manager Becker-Acroma, Professor **Anders Hult** of the Fibre and Polymer Technology department at KTH, and **Sonny Jönsson**, photopolymerization guru of former Becker-Acroma stature: They talked me into starting kinetics PhD research at Becker-Acroma.

The girls at the analysis lab, same company as before, **Sara, Martina** and **Karin**: Those where fun times... Sometimes I even met you during the days!†

Associate Professor **Mats Johansson** of the Fibre and Polymer Technology department at KTH: With his unending patience and optimism he has guided me when I have hit bare spots on the so spottily paved scientific road.

Cast in order of appearance, Colorado, USA:

Professor **Christopher Bowman** at Chemical and Biological Engineering, the University of Colorado: I first met Chris at a conference in Berlin and he said, come over for a post-doc. Instead it turned into a pre-doc. When I arrived at CU, he sat me down and asked me, so what do you want to do? He gave me three funded projects to pick from. One was on microfluidic devices. I thought, microfluidic what? That sounds exciting! I'll do that one. Two years later we were using the third generation CLiPP machinery to fabricate 3D polymeric devices, we had started a company and we had just finished the first project for Sandia National Labs. Who said research isn't exciting?!

Dear PhD student colleague (nice) Dr. **Brian Good**: To not like Brian is humanly impossible. Most of the devices presented in this thesis grew out of nothing on his blackboard. The designs, that is.

(Party) Dr. **Brian Hutchison**: A PhD student with very high standards. He examines and criticizes ideas with gusto. Many of the basic CLiPP concepts were discussed and rediscussed with Brian.

On a personal level, this would not have been possible without the never ending support and help of **Kristina**, my beloved wife.

† I worked nights quite a bit. Nothing else is implied.

Appendix A

Table A1: Overview of materials used in microfluidic device fabrication

Functional groups/Trade name	**UV-dose* (J/cm²)**	**Main features**	**Patterning**	**Drawbacks**
Acrylates	15-25	High Tg/Monomer availability	Good	Shrinkage
Methacrylates	20-30	High Tg/Monomer availability/grafting	Poor	Patterning
Thiol-enes	0.5-1.0	Rubbery-Medium high modulus/ low shrinkage-low residual stresses	Adequate	Stickiness/Rinsing of oligomers
Vinyl ether-maleates	1.0-3.0 (No TED)	Alternating polymerization/controlled residual functionality	Very Good	Poor mechanical properties
Kion Ceraset/Thiols	0.5-1.0 (No TED)	SiCN ceramics(after pyrolysis)	Good	Rinsing of oligomers
Allied Photochemical UVAG 0010	30+ heat, 80ºC for 10 min	Electrical conduction	Very poor	Has to be backfilled, only limited patterning possible
DuPont 7082	Physically drying	Filaments (i.e., resistance heating)	None	Physically drying

* 200 μm in the presence of TED, unless otherwise noted.

References

[1] T. Thorsen, S. Maerkl, S. Quake, Microfluidic large-scale integration, Science, 298, 580-584, 2002

[2] D. Duffy, H. Gillis, J., Lin, N. Sheppard, G. Kellogg, Microfabricated centrifugal microfluidic systems: Characterization and multiple enzymatic assays. Analytical Chemistry, 71, 4669-4678, 1999

[3] E. Eteshola, D. Leckband, Development and characterization of an ELISA assay in PDMS microfluidic channels, *Sensors and Actuators B-Chemical*, 72, 129-133, 2001.

[4] D. Pinto, Y. Ning, D. Figeys, An enhanced microfluidic chip coupled to an electrospray Qstar mass spectrometer for protein identification, Electrophoresis, 21 (1), 181-190, 2000

[5] L. Koutny, D. Schmalzing, O. Salas-Solano, S. El-Difrawy, A. Adourian, S. Buonocore, K. Abbey, P. McEwan ,P. Matsudaira, D. Ehrlich, Eight hundred base sequencing in a microfabricated electrophoretic device, Analytical Chemistry, 72, 3388-3391, 2000

[6] M. Madou, Fundamentals of Microfabrication: The Science of Miniaturization, 2nd Ed., CRC Press: Boca Raton, 2002

[7] T. Lagally, I. Medintz, R. Mathies, Single-molecule DNA amplification and analysis in an integrated microfluidic device, Analytical Chemistry, 73, 565-570, 2001

[8] H. Liu, M. Stremler, K. Sharp, M. Olsen, J. Santiago, R. Adrian, H. Aref, D. Beebe , Passive mixing in a three-dimensional serpentine microchannel, Journal of Microlecromechanical Systems, 9 (2), 190-197, 2000

[9] D. Stroock, S. Dertinger, A. Ajdari, I. Mezic , H. Stone , G. Whitesides, Chaotic mixer for microchannels Science, 295, 647-651, 2002

[10] J. Tice, A. Lyon, R. Ismagilov, Effects of viscosity on droplet formation and mixing in microfluidic channels, Analytica Chimica Acta, 507 (1), 73-77, 2004

[11] H. Simms, C. Brotherton, B. Good, R. Davis, K. Anseth, C. Bowman, In situ fabrication of macroporous polymer networks within microfluidic devices by living radical photopolymerization and leaching, Lab on a Chip, 5 (2), 151-157, 2005

[12] C. Hansen, E. Skordalakes, J. Berger, S. Quake, A robust and scalable microfluidic metering method that allows protein crystal growth by free interface diffusion, Proceedings of the National Academy of Sciences of the United States of America, 99 (26), 16531-16536, 2002

[13] J. Olofsson, K. Nolkrantz, F. Ryttsen, B. Lambie, S. Weber, O. Orwar, Single-cell electroporation, Current Opinion in Biotechnology 14 (1), 29-34, 2003

[14] P. Auroux, D. Iossifidis, D. Reyes, A. Manz, Micro total analysis systems. 2. Analytical standard operations and applications, Analytical Chemistry, , 74, 2637–2652, 2002

[15] D. Beebe, G. Mensing, G. Walker, Physics and applications of microfluidics in biology, Annual. Review of Biomedical Engineering, 2002, 4, 261–286.

[16] J. McDonald, G. Whitesides, Poly(dimethylsiloxane) as a material for fabricating microfluidic devices, Acc. Chem. Res. 2002, 35, 491–499.

[17] D. Figeys, Adapting arrays and lab-on-a-chip technology for proteomics, Proteomics, 2 (4), 373-382, 2002

[18] H. Becker, C. Gartner, Polymer microfabrication methods for microfluidic analytical applications, Electrophoresis 2000, 21, 12-26.

[19] H. Becker, L. Locascio, Polymer microfluidic devices, Talanta 2002, 56, 267-287.

[20] G. Liu, Y. Tian, Y. Kan, Fabrication of high-aspect-ratio microstructures using SU8 photoresist, Microsystem Technologies-Micro-and Nanosystems-Information Storage and Processing Systems, 11, (4-5), 343-346, 2005

[21] F. Tseng, K. Lin, H. Hsu, C. Chieng, A surface-tension-driven fluidic network for precise enzyme batch-dispensing and glucose detection, Sensors and Actuators A-Physical, 111 (1), 107-117 2004

[22] Y. Xia, G. Whitesides, Soft Lithography, Annual Review of Materials Science, 28, 153-184, 1998

[23] D. Beebe, J. Moore, Q. Yu, R. Liu, M. Kraft, B. Jo C., Devadoss, Proceedings of the National Academy of Sciences of the United States of America, 97, 13488-13493, 2000

[24] V. Studer, A. Pepin, Y. Chen, Nanoembossing of thermoplastic polymers for microfluidic applications, Applied Physics Letters, 80 (19) 3614-3616 2002

[25] H. Schift, R. Jaszewski, C. David , J. Gobrecht, Nanostructuring of polymers and fabrication of interdigitated electrodes by hot embossing lithography, Microelectronic Engineering, 46 (1-4), 121-124, 1999

[26] J. Narasimhan, I. Papautsky, Polymer embossing tools for rapid prototyping of plastic microfluidic devices, Journal of Micromechanics and Microengineering, 14 (1) 96-103, 2004

[27] E. Yablonovitch, R. Vrijen, Optical projection lithography at half the Rayleigh resolution limit by two-photon exposure, Optical Engineering, 38 (2), 334-338, 1999

[28] E. Stenberg, B. Persson, H. Roos, C. Urbanicky, Quantitative-Determination of Surface Concentration of Protein With Surface-Plasmon Resonance using Radiolabeled Proteins, Journal of Colloid and Interface Science, 143 (2), 513-526, 1991

[29] S. Hu, W. Brittain, Surface grafting on polymer surface using physisorbed free radical initiators, Macromolecules, 38 (15), 6592-6597, 2005

[30] D. Trimbach, K. Feldman, N. Spencer, D. Broer, C. Bastiaansen , Block copolymer thermoplastic elastomers for microcontact printing, Langmuir 19 (26), 10957-10961, 2003

[31] K. Choi, J. Rogers, A Photocurable Poly(dimethylsiloxane) Chemistry Designed for Soft Lithographic Molding and Printing in the Nanometer Regime, Journal of the American Chemical Society, 125(14) 4060 – 4061, 2003

[32] J. Beebe, J. Moore, Microfabricated devices and method of manufacturing the same, United States Patent 6,488,872, 2002

[33] J. Moorthy, G. Mensing , D. Kim, S. Mohanty, D. Eddington, W. Tepp, E. Johnson, D. Beebe, Microfluidic tectonics platform: A colorimetric, disposable botulinum toxin enzyme-linked immunosorbent assay system, Electrophoresis, 25 (10-11), 1705-1713, 2004

[34] G. Odian, Principles of Polymerization, 3rd ed. New York: John Wiley & Sons Inc., 1991

[35] T. Endo, W. Bailey, Radical Ring-Opening Polymerization of 3,9-Dimethylene-1,5,7,11-Tetraoxaspiro-[5,5]Undecane, Journal of Polymer Science Part C-Polymer Letters, 13 (4), 193-195, 1975

[36] C. Hoyle, R. Hensel, M. Grubb, Laser-Initiated Polymerization of a Thiol-Ene System, Polymer Photochemistry, 4 (1), 69-80, 1984

[37] D. Smith, Journal of Applied Chemistry, 17, p342, 1967

[38] H. Tobita, Kinetics of Free-Radical Polymerization with Chain-Length-Dependent Bimolecular Termination under Unstationary Conditions, Macromolecules, 29, 3073-3080, 1996

[39] T. Scherzer, U. Decker, Kinetic investigations on the UV-induced photopolymerization of a diacrylate by time-resolved FTIR spectroscopy: the influence of photoinitiator concentration, light intensity and temperature, Radiation Physics and Chemistry, 55 (5-6), 615-619, 1999

[40] J. Miller, J. Miller, Statistics for analytical chemistry, 3rd edition, Chichester: Ellis Horwood Ltd., 1993

[41] K. Berchtold, L. Lovell, J. Nie, B. Hacioglu, C. Bowman, The significance of chain length dependent termination in cross-linking polymerizations, Polymer, 42 (11), 4925-4929, 2001

[42] K. Berchtold, T. Lovestead, C. Bowman, Coupling chain length dependent and reaction diffusion controlled termination in the free radical polymerization of multivinyl (meth)acrylates, Macromolecules, 35 (21), 7968-7975, 2002

[43] G. Litvinenko, V. Kaminsky, Role of Diffusion-Controlled Reactions in Free-Radical Polymerization, Progress in Reaction Kinetics, 19 (2), 139-193, 1994

[44] S. Zhu, A. Hamielec, Chain-Length-Dependent Termination For Free-Radical Polymerization, Macromolecules, 22 (7), 3093-3098,1998

[45] G. Smith, G. Russell, M. Yin, J. Heuts, The effects of chain length dependent propagation and termination on the kinetics of free-radical polymerization at low chain lengths, European Polymer Journal, 41 (2), 225-230, 2005

[46] T. Lovestead, K. Berchtold, C. Bowman, Modeling the effects of chain length on the termination kinetics in multivinyl photopolymerizations, Macromolecular Theory and Simulation,11,729-738, 2002

[47] C. Decker, C. Bianchi, D. Decker, F. Morel, Photoinitiated polymerization of vinyl ether-based systems, Progress in Organic Coatings, 42 (3-4), 253-266, 2001

[48] J. Jansen, E. Houben, P. Tummers, D. Wienke, J. Hoffmann, Real-time infrared determination of photoinitiated copolymerization reactivity ratios: Application of the Hilbert transform and critical evaluation of data analysis techniques, Macromolecules, 37 (6), 2275-2286, 2004

[49] G. Moad, D. Solomon, The Chemistry of Radical Polymerizations, 2nd edition, Elsevier, 2005

[50] B. Yamada, E. Yoshikawa, T. Otsu, Steric Environments of Radicals Produced by Addition of Tert-Butoxyl Radicals to Dialkyl Maleates as Studied by Spin Trapping With 2,4,6-Tri-Tert-Butyl-1-Nitrosobenzene, Macromolecular Chemistry and Physics, 192 (9), 1931-1940, 1991

[51] C. Decker, Photoinitiated Curing of Multifunctional Monomers, Acta Polymerica, 45 (5), 333-347, 1994

[52] C. Decker, F. Morel, S. Jonsson, S. Clark, C. Hoyle, Light-induced polymerisation of photoinitiator-free vinyl ether maleimide systems, Macromolecular Chemistry and Physics, 200 (5), 1005-1013, 1999

[53] B. Rånby, J. Rabek, ESR Spectroscopy in Polymer Research, Springer-Verlag, New York, 1977

[54] C. Decker, D. Decker, F. ,Morel, Light intensity and temperature effect in photoinitiated polymerization, Photopolymerization ACS Symposium Series, 673, 63-80, 1997

[55] A. Stolov, T. Xie, J. Penelle, S. Hsu, H. Stidham, An analysis of photopolymerization kinetics and stress development in multifunctional acrylate coatings, Polymer Engineering and Science, 41 (2) 314-328, 2001

[56] A. Stolov, T. Xie, J. Penelle, S. Hsu, Stress buildup in ultraviolet-cured coatings: Sample thickness dependence, Macromolecules 34 (9) 2865-2869, 2001

[57] J. Payne, F. Francis, A. McCormick, The effect of processing variables on stress deveopment in ultraviolet-cured coatings, Journal of applied polymer sciences, 66, 1627-1277, 1997

[58] N. Luo, J. Hutchison, K. Anseth, C. Bowman, Synthesis of a novel methacrylic monomer and its application in surface photografting on crosslinked polymeric substrates, Journal of Polymer Science Part A Polymer Chemistry, 40, 1885-1891, 2002.

[59] N. Pamme, R. Koyama, A. Manz, Counting and sizing of particles and particle agglomerates in a microfluidic device using laser light scattering: application to a particle-enhanced immunoassay, Lab on a Chip, 3 (3), 187-192, 2003

[60] N. Jeon, D. Chiu, C. Wargo, H. Wu, I. Choi, J. Anderson, G. Whitesides, Design and fabrication of integrated passive valves and pumps for flexible polymer 3-dimensional microfluidic systems, Biomedical Microdevices, 4 (2) 117-121, 2002

[61] E. Hasselbrink, T. Shepodd, J. Rehm, High-pressure microfluidic control in lab-on-a-chip devices using mobile polymer monoliths, Analytical Chemistry, 74 (19), 4913-4918 2002

[62] M. Powers, K. Domansky, M. Kaazempur-Mofrad, A. Kalezi, A. Capitano, A. Upadhyaya, P. Kurzawski, K. Wack, D. Stolz, R. Kamm, L. Griffith, A microfabricated array bioreactor for perfused 3D liver culture, Biotechnology and Bioengineering, 78 (3) 257-269, 2002

[63] T. von Werne, D. Germack, C. Hagberg, W. Sheares, C. Hawker, K. Carter, A versatile method for tuning the chemistry and size of nanoscopic features by living free radical polymerization, Journal of the American Chemical Society, 125 (13) 3831-3838, 2003

[64] N. Luo, J. Hutchison, K. Anseth, C. Bowman, Synthesis of a novel methacrylic monomer and its application in surface photografting on crosslinked polymeric substrates, Journal of Polymer Science Part A Polymer Chemistry,. 40, 1885–1891, 2002

[65] S. Reddy, R. Sebra, K. Anseth, C. Bowman, Living radical photopolymerization induced grafting on thiol-ene based substrates, Journal of Polymer Science Part A Polymer Chemistry, 10, 2134-2144, 2005

[66] Personal communication, Sirish Reddy at the Department of Biological and Chemical Engineering, University of Colorado, 2005

[67] J. Brandrup, E. Immergut, E. Grulke, Polymer Handbook, 4th Edition Wiley-Interscience, Chapter VI, 1999

[68] Personal communication, Sirish Reddy at the Department of Biological and Chemical Engineering, University of Colorado, 2005

[69] Personal communication, Sirish Reddy at the Department of Biological and Chemical Engineering, University of Colorado, 2005

[70] P. Passeraub, A. Almeida, and N. Thakor, Design, microfabrication and characterization of a microfluidic chamber for the perfusion of brain tissue slices, Biomedical Microdevices, 5, 147-155, 2003.